

Back to Belgium Grants

Final Report

Name of the researcher	DECLEVES Anne-Emilie
Selection Year	2012/2013
Host institution	ULB – Laboratoire de Néphrologie Expérimentale
Supervisor	Pr. Joëlle Nortier
Period covered by this report	from 01/03/2014 to 01/01/2016
Title of the project	Endothelial and vascular dysfunctions in Aristolochic Acid Nephropathy. Role of AMP-activated protein kinase.

1. Objectives of the proposal (1 page)

During this postdoc research, I was mainly involved on the signalling pathway connecting oxidative stress, mitochondrial dysfunction and energy challenges in a model of Aristolochic Acid (AA) nephropathy. Furthermore, my postdoc position at ULB allowed me to complete several work in another experimental model: the high-fat diet-induced kidney injury in mice.

AAN is a progressive chronic tubulointerstitial disease characterized by cortical tubular atrophy, dense tubulointerstitial fibrosis with relatively well preserved glomeruli. In patient, AAN was characterized by a rapid deterioration in renal function, with initial serum creatinine doubling within about 3 months leading to ESRD. Glomerular injury and tubulointerstitial damages, including tubular atrophy as well as interstitial fibrosis, are determinant to the evolution of ESRD. Despite the US Food and Drug Administration alert regarding the safety of botanical remedies containing AA (known or suspected to contain AA), plants containing AA are still available via the Internet. Therefore, further knowledge is necessary to elucidate the pathways of AA-induced nephropathy. From clinical to experimental studies, Dr. Nortier's team has been achieving outstanding works to increase the knowledge in the pathophysiology of AAN; demonstrating structural and functional impairment of the proximal tubules. Its experimental work also highlighted that AA-induced nephropathy consists in a biphasic evolution with an acute phase (3-10 days) characterized by the impairment of the proximal tubules associated with proteinuria followed by a chronic phase (after 14 days) characterized by a progressive development of the interstitial fibrosis. However, a full understanding of mechanisms involved to the AAN is still absent, especially regarding to the mitochondrial challenge and vascular feature. Therefore, in our proposal, we planned to extend the knowledge in to essential questions regarding the response of the kidney to the AA exposure in the concept of relationship between vascular dysfunctions and progressive renal disease.

2. Methodology and Results

Study 1. We focused on nitric oxide (NO). Indeed, a reduced NO bioavailability were previously described in a rat model of AAN. Moreover, NO deficiency has been shown to play a key role in other kidney diseases. To further explore the role of NO in our model, we decided to restore renal NO bioavailability using L-Arginine (L-Arg) supplementation.

Acute kidney injury (AKI) is a common clinical issue associated with high morbidity and mortality rates. Moreover, even a short AKI episode can lead to subsequent long term complications, including the progression to chronic kidney disease (CKD) or end-stage renal disease. These complications are

usually associated to incomplete tubular repair, persistent tubulointerstitial inflammation and endothelial dysfunction, and excessive accumulation of extracellular matrix. Nowadays, there is an urgent need to better understand the pathological processes that lead to AKI-to-CKD complications. AAN, a progressive tubulointerstitial injury of toxic origin, is characterized by early and transient acute tubular necrosis, followed by fibrosis and tubular atrophy leading to loss of renal function. A reduced NO production has been demonstrated, which may disturb the regulation of renal function. The present study tested the hypothesis that L-arginine supplementation may restore renal function and reduce renal injury after AA intoxication. To investigate this, C57BL/6J male mice were randomly subjected to ip injection of either sterile saline solution (control) or AAI (2,5mg/Kg) for 5 days. To determine if the renal AA-induced injuries were related to NO reduction, L-Arginine (L-Arg), a substrate for NO synthase, was supplemented in drinking water. Mice intoxicated with AAI displayed polyuria, significantly increased plasma creatinine level, glycosuria, proteinuria and FE_{Na^+} ($P<0.05$) along with severe proximal tubular cell necrosis, renal inflammation and increased oxidative stress ($P<0.05$). These lesions were associated with a significant reduction of NO bioavailability. L-Arg supplementation in AA-treated mice significantly improved overall kidney function, as reported by reduced urine volume, plasma creatinine level, proteinuria and FE_{Na^+} ($P<0.05$) in in AAI+L-Arg-treated mice. Moreover, L-Arg treatment resulted in a significant reduction of tubular cell necrosis, and reduced renal inflammation and oxidative stress along with a normalized NO bioavailability. Interestingly, these AAI-induced renal impairments were associated with a significant increase in NOX2 expression while NOX1 and NOX4 expressions did not change. This rise was also prevented by the L-Arg supplementation. Therefore, it seems that NO is a key mediator of renal function in AAN. These results showed that a preservation of the NO concentration by L-Arg supplementation leads to a kidney protection in AA-induced nephropathy. Moreover, we showed for the first time that NADPH oxidase might be involved in the AAN.

This study was published in *Experimental Physiology* (“*Protective effect of nitric oxide in aristolochic acid-induced toxic acute kidney injury: an old friend with new assets*” Anne-Émilie Declèves, Inès Jadot, Vanessa Colombaro, Blanche Martin, Virginie Voisin, Isabelle Habsch, Éric De Prez, Joëlle Nortier, Nathalie Caron. *Exp Physiol* 2016, 101.1, 193-206) (**Annex I**).

Another ongoing study has been starting with a PhD student to further determine the effect of L-Arginine in the transition to acute kidney injury to chronic kidney injury. Since the severity of AKI is associated with the progression to advanced CKD, we are evaluating the impact of L-Arg supplementation on the AA-induced AKI-to-CKD transition. The results showed an interesting beneficial effect of L-Arginine on tubular injury and fibrosis. The data are included in a “in progress” manuscript (“*L-Arginine supplementation improves chronic kidney injury in experimental aristolochic acid nephropathy*”) that should be submitted in October.

Study 2. Endothelial and vascular dysfunctions in Aristolochic Acid Nephropathy. Role of AMP-activated protein kinase

In this project, the pathological link between tubular and endothelial dysfunctions and the AMPK activation has been targeted. AMPK is a central energy sensor of the cell that has been characterized in the kidney. It plays a critical role in cellular responses to low energy levels by switching off pathways that consume energy and switching on those that produce it. Moreover, in order to better understand the phenomena of AKI-to-CKD transition, the experimental protocol was designed at two different time-points, an acute time-point (Day 5) and a chronic time-point (Day 20). Therefore, mice were treated either with vehicle sterile saline solution, AAI solution (i.p. - 2.5 mg/kg) or AAI+AICAR, the specific AMPK activator (5-Aminoimidazole-4-carboxamide-1- β -D-ribofuranoside - i.p. at 0.5 mg/g b.w.). For the Short-term Study, mice received 4 daily injections and

were euthanized on Day 5. In contrast, for the Long-term Study, mice received 4 daily injections but were maintained until Day 20.

AA-treated mice displayed loss of renal function, as reflected by significant increases in plasma creatinine level and proteinuria at days 5 and 20. In addition, impairment of tubular cells was also observed by the significant increase in urinary excretion of lysosomal enzyme N-acetyl- β -D-glucosaminidase in AA-treated mice. These changes were prevented by AICAR treatment. To further determine the role of AMPK in AA-induced oxidative stress, Nox1, 2 and 4 were investigated at the mRNA levels. No changes were observed for Nox1 and 4. However, Nox2 was significantly increased in AA-treated mice while this rise was prevented by AICAR treatment at day 5 but not at day 20. Moreover, the urinary hydrogen peroxide level, a stable product of ROS production, was significantly higher after AA intoxication and reduced with AICAR. Regarding inflammation, AA mice exhibited a significant increase in MCP-1 mRNA level. This rise was only prevented by AICAR at day 5. Finally, at day 5, there was no significant macrophage infiltration with AICAR while at day 20, this significant increase was not prevented by AICAR.

These findings show a beneficial effect of AMPK in AA-induced AKI. In view of these data, we suggest that chronic AICAR treatment is necessary for complete nephroprotection and recovery. The activation of AMPK represents a potential strategy to prevent the transition from AKI-to-CKD.

These data were presented at the annual meeting of the American Society of Nephrology, San Diego, CA, USA in last November (**Annex II**). The data are included in a “in progress” manuscript.

Study 3. Targeted metabolomics of plasma samples in AA-induced nephropathy. Finally, in parallel, we completed a metabolomic analysis in plasma samples. This was in collaboration with Pr. K. Sharma (Director of Center for Renal Translational Medicine at UCSD) and Pr. B. Naviaux (Professor of Genetics Biochemical Genetics and Metabolism AND Co-director of The Mitochondrial and Metabolic Disease Center, UCSD).

In order to better explore the pathogenesis of AAN, a targeted metabolomic analysis was performed in plasma of AA-intoxicated mice. In addition, the effect of AMP-activated Protein Kinase (AMPK) activation with AICAR was also investigated.

C57BL/6J male mice were randomly subjected to i.p. injection of either sterile saline solution, AA, AA+AICAR, the specific AMPK activator for 4 days. Mice were then euthanized at day 5. Targeted metabolites were detected in plasma using an AB SCIEX QTRAP 5500 triple quadrupole mass spectrometer equipped with a Turbo V electrospray ionization (ESI) source, and Shimadzu LC-20A UHPLC system. Results revealed that, from 582 metabolites targeted, 217 metabolites were below limit of quantitation and 365 metabolites were detected. Based on the VIP Score, 30 metabolites were dysregulated in this acute phase of the experimental AAN model. Among them, 23 metabolites were significantly increased in AA-treated mice and 7 were significantly decreased (Table 1). AICAR treatment ameliorated the change of 15 of these metabolites (Table 2). Among the observed changes, several metabolic pathways were affected, in particular gut microbiome metabolism, liver and bile acid metabolism, tryptophan metabolism, purine and pyrimidine metabolism and mitochondrial metabolism. Tryptophan-derived metabolites considered as uremic toxin such as xanthurenic acid, kynurenic acid were increased in AA-treated mice and reduced with AICAR.

These metabolomic approach provided novel findings regarding early perturbations occurring in metabolic pathways in AAN. Moreover, our results suggest 1) a crosstalk between gut microbiome and kidney, especially in relation with tryptophan metabolism and accumulation of uremic toxins; 2) a beneficial role of AMPK in reducing the level of uremic toxins.

Table 1.		
SHAM - Low		SHAM - High
AAI - High		AAI - Low
Hippuric Acid		Pyrophosphate
Tetrahydrobiopterin		Taurocholic Acid
Kynurenic Acid		Taurodeoxycholic Acid
2-Isopropylmalic Acid		Propionylcarnitine
Shikimic Acid		Melatonin
2-Pyrocatechuic Acid		Glycocholic Acid
Trimethylamine		Taurochenodesoxycholic Acid
Chenodeoxyglycholic Acid		
L-Ascorbic Acid		
2-deoxyglucose-6-phosphate		
Xanthurenic Acid		
creatinine		
Salicyluric Acid		
Pyridoxal		
3-hydroxyanthranillic Acid		
Allantoine		
Ureidosuccinic Acid		
Uridine		
N-acetylserine		
2-keto-L-gluconate		
CoQ9H2		
1-Methyladenosine		
Imidazoleacetic Acid		

Table 2.		
SHAM - Low		SHAM - High
AAI + AICAR - moderate		AAI + AICAR - moderate
AAI - High		AAI - Low
Kynurenic Acid		Taurodeoxycholic Acid
2-Isopropylmalic Acid		Taurochenodesoxycholic Acid
2-Pyrocatechuic Acid		
Trimethylamine		
Chenodeoxyglycholic Acid		
L-Ascorbic Acid		
2-deoxyglucose-6-phosphate		
Xanthurenic Acid		
creatinine		
Salicyluric Acid		
Pyridoxal		
3-hydroxyanthranillic Acid		
Ureidosuccinic Acid		

These data were presented at the annual meeting of the American Society of Nephrology, San Diego, CA, USA in last November (**Annex III**).

4. Valorisation/Diffusion (including Publications, Conferences, Seminars, Missions abroad...)

This grant allowed me:

(1) to write 6 peer-reviewed original articles and 2 invited reviews that I have been accepted in high-level scientific journals as well as to participate to several others studies from collaborators and sign as co-authors in 12 other publications

1. Pozdzik AA, Giordano L, Li G, Antoine MH, Quellard N, Godet J, De Prez E, Husson C, Declèves AE, Arlt VM, Goujon JM, Brochériou-Spelle I, Ledbetter SR, Caron N, Nortier JL. **Blocking TGF- β Signaling Pathway Preserves Mitochondrial Proteostasis and Reduces Early Activation of PDGFR β + Pericytes in Aristolochic Acid Induced Acute Kidney Injury in Wistar Male Rats**. PLoS One. 2016 Jul 5;11(7): e0157288
2. Miyamoto S, Hsu CC, Hamm G, Darshi M, Diamond-Stanic M, Declèves AE, Slater L, Pennathur S, Stauber J, Dorrestein PC, Sharma K. **Mass Spectrometry Imaging Reveals Elevated Glomerular ATP/AMP in Diabetes/obesity and Identifies Sphingomyelin as a Possible Mediator**. EBioMedicine. 2016 May; 7: 121-34.
3. Declèves AE, Jadot I, Colombaro V, Martin B, Voisin V, Habsch I, De Prez E, Nortier J, Caron N. **Protective effect of nitric oxide in aristolochic acid-induced toxic acute kidney injury. An old friend with new assets**. Exp. Physiol. 2016 Jan; 101(1): 193-206.
4. Colombaro V, Jadot I, Declèves AE, Voisin V, Giordano L, Habsch I, Malaisse J, Flamion B, Caron N. **Lack of hyaluronidases exacerbates renal post-ischemic injury, inflammation, and fibrosis**. Kidney Int. 2015 Jul; 88(1): 61-71.
5. Antoine MH, Debelle F, Piccirilli J, El Kaddouri F, Declèves AE, De Prez E, Husson C, Mies F, Bourgeade MF, Nortier JL. **Human bone morphogenetic protein-7 does not counteract aristolochic acid-induced renal toxicity**. J Appl Toxicol. 2015 Dec; 35(12): 1520-1530.
6. Robbe A, Tassin A, Carpentier J, Declèves AE, Ngono ZL, Nonclercq D, Legrand A. **Intratracheal bleomycin aerosolization: the best route of administration for a scalable and homogeneous pulmonary fibrosis rat model?** BioMedical research International. 2015 Jan
7. Declèves AE, Sharma K, Satriano J. **Beneficial Effects of AMP-Activated Protein Kinase Agonists in Kidney Ischemia-Reperfusion: Autophagy and Cellular Stress Markers**. Nephron Exp Nephrol. 2014 Dec 6.
8. Declèves AE, Sharma K. **Obesity and kidney disease: differential effects of obesity on adipose tissue and kidney inflammation and fibrosis**. Curr Opin Nephrol Hypertens. 2015 Jan; 24(1):28-36.

9. Colombaro V, Jadot I, Declèves AE, Voisin V, Giordano L, Habsch I, Flamion B, Caron N. **Hyaluronidase 1 and hyaluronidase 2 are required for renal hyaluronan turnover.** Acta Histochem. 2015 Jan; 117(1):83-91.
10. Voisin V, Declèves AE, Hubert V, Colombaro V, Giordano L, Habsch I, Bouby N, Nonclercq D, Caron N. **Protection of Wistar-Furth rats from post-ischemic acute renal injury: a role for Nitric Oxide and Thromboxane?** Clin Exp Pharmacol Physiol. 2014 Nov; 41(11):911-20.
11. Borsting E, Patel SV, Declèves AE, Lee SJ, Rahman QM, Akira S, Satriano J, Sharma K, Vallon V, Cunard R. **Tribbles Homolog 3 Attenuates Mammalian Target of Rapamycin Complex-2 Signaling and Inflammation in the Diabetic Kidney.** J Am Soc Nephrol. 2014 Sep;25(9):2067-78.
12. Declèves AE, Sharma K. **Novel targets of antifibrotic and anti-inflammatory treatment in CKD.** Nat Rev Nephrol. 2014 May; 10(5):257-67.
13. Declèves AE, Zolkipli Z, Satriano J, Wang L, Nakayama T, Rogac M, Le TP, Nortier JL, Farquhar MG, Naviaux RK, Sharma K. **Regulation of lipid accumulation by AMP-activated kinase [corrected] in high fat diet-induced kidney injury.** Kidney Int. 2014 Mar; 85(3):611-23. doi: 10.1038/ki.2013.462. Epub 2013 Dec 4. Erratum in: Kidney Int. 2014 Jun; 85(6):1474.
14. Declèves AE, Pozdzik AA, Baudoux T, Habsch I, De Prez E, Flamion B, Nortier JL, Caron N. **CD44-positive cells and hyaluronan are a hallmark of a rat model of aristolochic acid nephropathy.** J Cytol Histol. 2013; 4:4 [under press]
15. Dugan LL, You YH, Ali SS, Diamond-Stanic M, Miyamoto S, Declèves AE, Andreyev A, Quach t, Ly S, Shekhtman G, Nguyen W, Chepetan A, Le TP, Wang L, Xu M, Paik KP, Fogo A, Viollet B, Murphy A, Brosius F, Naviaux RK, Sharma K. **AMPK dysregulation promotes diabetes-related reduction of superoxide and mitochondrial function.** J Clin Invest. 2013 Nov 1; 123 (11): 4888-4899.
16. Declèves AE, Rychak JJ, Smith DJ, Sharma K. **Effect of high-fat diet and losartan on renal cortical blood flow using contrast ultrasound imaging.** Am J Physiol Renal Physiol. 2013 Nov; 305 (9): F1343-51.
17. Colombaro V, Declèves AE, Jadot I, Voisin V, Giordano L, Habsch I, Nonclercq D., Flamion B., Caron N. **Inhibition of hyaluronan is protective against renal ischaemia-reperfusion injury.** Nephrol Dial Transplant. 2013 Oct; 28 (10): 2484-2493.
18. Hu X, Mahakian LM, Caskey CF, Beegle JR, Kruse DE, Declèves AE, Sharma K, Rychak JJ, Sutcliffe P, Ferrara KW. **In vivo validation and 3D visualization of broadband ultrasound molecular imaging.** Am J Nucl Med Mol Imaging. 2013 Jul 10; 3(4): 336-349.
19. Lee SJ, Borsting E, Declèves AE, Singh P, Cunard R. **Podocytes Express IL-6 and Lipocalin 2/ Neutrophil Gelatinase-Associated Lipocalin in Lipopolysaccharide-Induced Acute Glomerular Injury.** Nephron Exp Nephrol. 2012 Dec 8; 121(3-4): e86-e96

20. Declèves AE, Caron N, Voisin V, Legrand A, Bouby N, Kultti A, Tammi ML, Flamion B. **Two-step fragmentation of hyaluronan in renal ischemia**. *Nephron Dial Transplant*. 2012 Oct; 27 (10): 3771-81.

(2) to attend several national and international meetings

2015: Annual meeting of the American Society of Nephrology, San Diego, CA, USA.

Poster 1: Evaluation of iNOS Inhibition on Kidney Functions in High-Fat Diet-Induced Obesity. AE Declèves, B Martin, V Colombaro, I Jadot, I Habsch, JL Nortier and N Caron.

Poster 2: Implication of AMPK Activation in Experimental Aristolochic Acid Nephropathy: Use of a Targeted Metabolomic Analysis. AE Declèves, I Jadot, V Colombaro, K Li, N Caron, JL Nortier and RK Naviaux.

Poster 3: Role of AMPK in Aristolochic Acid-Induced Acute Kidney Injury. AE Declèves, I Jadot, V Colombaro, E De prez, I Habsch, K Sharma, N Caron and JL Nortier

2015: 27th Annual Meeting of the European Renal Cell Study Group (ERCSCG), Ireland.

Oral communication: Effects of aristolochic acids on cultured endothelial cells (EAhy926). AE Declèves, MH Antoine, C Husson, C Fontaine, S Stévigny, J Nortier

2014: 51st ERA-EDTA Congress, Amsterdam, The Netherlands.

Poster : Enhanced nitric oxide production ameliorates acute kidney injury in experimental aristolochic acid nephropathy. I Jadot, AE Declèves, V Colombaro, B Martin, V Voisin, I Habsch, E De Prez, J Nortier, N Caron

2014: Belgian Society of Nephrology, Genk, Belgium

Poster: Enhanced nitric oxide production ameliorates acute kidney injury in experimental aristolochic acid nephropathy. I Jadot, AE Declèves, V Colombaro, B Martin, V Voisin, I Habsch, E De Prez, J Nortier, N Caron

2012: Annual meeting of the American Society of Nephrology, San Diego, CA, USA.

Poster: Lipidomic Analysis of Kidney Tissue in a High-Fat Diet Model: A Key Role of AMPK in Lipid Content and Storage. AE Declèves, J Satriano, Z Zolkipli, A Thomas, J Nortier, M Farquhar, DD Sears, E Dennis, O Quehenberger, RK Naviaux, K Sharma

2012: Benelux Kidney Meeting, Eindhoven, The Netherlands.

Poster 1: Cross-Talk between CD44+ Cells and Hyaluronan in a Rat Model of Aristolochic Acid Nephropathy. AE Declèves, AA Pozdzik, L Giordano, E De Prez, B Flamion, N Caron and JL Nortier

Poster 2: Endothelial cell toxicity induced in vitro by aristolochic acid is attenuated by anti-transforming growth factor-beta antibody (1D11). MH Antoine, A Jayaswal, R Redjed, C Husson, AE Declèves, L Giordano, T Baudoux, N Caron, T Roumequere, S Ledbetter, AA Pozdzik and JL Nortier

(3) to maintain my collaboration with University of California, San Diego (UCSD) and both **Professor Kumar Sharma**, MD, PhD, Director of Center for Renal Translational Medicine and **Professor Robert K. Naviaux**, MD, PhD, Co-director of The Mitochondrial and Metabolic Disease Center.

I went many times to UCSD in order to set up a targeted metabolomics analysis to study the implication of AMPK in our experimental aristolochic acid mouse model.

(4) to be co-PI and PI for PhD students in biomedical sciences

5. Future prospects for a permanent position in Belgium

Here is what I wrote in 2012 when I applied for this “return grant”:

“Give a short description of your career perspectives after your mandate

I am a postdoctoral researcher in nephrology. I just completed a three years’ postdoctoral research in Center for Renal Translational Medicine (Division of Nephrology) in University of California San Diego. In the next few years, I hope to strengthen my knowledge of experimental nephrology. I propose take trainings and courses in molecular pathology, in system biology (associated to lipidomics analysis) as well as statistical basis of research in these areas. I hope to merge collaborations with eminent researchers in the field to able to produce research findings that will make significant difference in treatment and understanding of kidney disease. In the next five years, I would like to be involved in transdisciplinary research projects in the field of experimental nephrology. By making the link between clinicians, physiologists and molecular biologists, I feel that I could develop translational research in nephrology between University of California San Diego and Université Libre de Bruxelles. Finally, I expect to be senior researcher in renal physiology and physiopathology, especially in developing specific original areas of interest such as the lipidomic analysis and system biology tools. In the long term, I hope to serve as a role model to aspiring women in the field of nephrology and mentor young researchers in to successful careers. Funding from Belgian federal Science Policy would give me the protected time and funding to build my publication profile to apply for independent grants. This would be a major step towards my future career aspirations.”

Four years later, I have been hired as senior lecturer and director of the laboratory of molecular biology. Position that I am still occupying ;)

6. Miscellaneous

I would like to very much thank the ‘Belspo return grant’ program for their help. It is with a real pleasure that I will now be an alumni and I am looking forward to helping new young research giving them advice and sharing the benefit of my experience.

Research Paper

Protective effect of nitric oxide in aristolochic acid-induced toxic acute kidney injury: an old friend with new assets

Anne-Émilie Declèves^{1,2}, Inès Jadot¹, Vanessa Colombaro¹, Blanche Martin¹, Virginie Voisin¹, Joëlle Nortier² and Nathalie Caron¹

¹Molecular Physiology Research Unit-URPHYM, University of Namur (UNamur), B-5000 Namur, Belgium

²Laboratory of Experimental Nephrology, Faculty of Medicine, Université Libre de Bruxelles (ULB), B-1070 Brussels, Belgium

New Findings

- **What is the central question of this study?**
Despite the fact that the pathogenesis of aristolochic acid (AA) nephropathy is still unclear, we sought to determine whether nitric oxide is involved in the underlying mechanism of AA-induced acute kidney injury (AKI).
- **What is the main finding and its importance?**
Using a model of progressive tubulointerstitial nephritis, in which AA nephropathy exhibits two interconnected phases, an acute phase and a chronic phase of injury, we demonstrated that maintenance of nitric oxide bioavailability is essential to improve the outcome of AA-induced AKI.

Aristolochic acid (AA) nephropathy (AAN), a progressive tubulointerstitial injury of toxic origin, is characterized by early and transient acute tubular necrosis. This process has been demonstrated to be associated with reduced nitric oxide (NO) production, which can disrupt the regulation of renal function. In this study, we tested the hypothesis that L-arginine (L-Arg) supplementation could restore renal function and reduce renal injury after AA intoxication. C57BL/6 J male mice were randomly subjected to daily i.p. injection of either sterile saline solution or AA (2.5 mg kg⁻¹) for 4 days. To determine whether AA-induced renal injuries were linked to reduced NO production, L-Arg, a substrate for NO synthase, was supplemented (5%) in drinking water. Mice intoxicated with AA exhibited features of rapid-onset acute kidney injury, including polyuria, significantly increased plasma creatinine concentrations, proteinuria and fractional excretion of sodium ($P < 0.05$), along with severe proximal tubular cell injury and increased NADPH oxidase 2 (Nox2)-derived oxidative stress ($P < 0.05$). This was associated with a significant reduction in NO bioavailability. L-Arg supplementation in AA-treated mice significantly increased NO bioavailability, which in turn improved renal function (creatininaemia, polyuria, proteinuria, fractional excreted sodium and N-acetyl- β -D-glucosaminidase enzymuria) and renal structure (tubular necrosis and tubular cell apoptosis). These changes were associated with significant reductions in Nox2 expression and in production of reactive oxygen species and with an increase in antioxidant concentrations.

A.-É. Declèves and I. Jadot contributed equally to this work.

There has been a change to the author listing since publication of the Accepted article version on Wiley Online Library (wileyonlinelibrary.com) on 7th October 2015.

Our results demonstrate that preservation of NO bioavailability leads to renal protection in AA-induced acute kidney injury by reducing oxidative stress and maintaining renal function.

(Received 16 May 2015; accepted after revision 30 September 2015; first published online 7 October 2015)

Corresponding author A.-É. Declèves: Laboratory of Experimental Nephrology, Faculty of Medicine, Université Libre de Bruxelles, Route de Lennik, 808, 1070 Brussels, Belgium. Email: anne-emilie.decleves@ulb.ac.be

Introduction

Aristolochic acid nephropathy (AAN) is a progressive tubulointerstitial (TI) injury of toxic origin caused by exposure to aristolochic acid (AA). Aristolochic acid nephropathy was originally reported in 1992 in young Belgian women after ingestion of slimming pills containing root extracts of *Aristolochia* sp. (Vanherweghem *et al.* 1993). Since then, many investigations have revealed new cases of nephropathy associated with the consumption of AA (Grollman *et al.* 2007; Debelle *et al.* 2008), particularly in Asian countries where AA is still used in traditional medicines. Therefore, AAN is considered to be a worldwide health concern with a substantial incidence (Debelle *et al.* 2008). Clinically, AAN is characterized by progressive proximal tubular atrophy and dense TI fibrosis that result in rapid deterioration of renal function, leading to end-stage renal disease (Vanherweghem *et al.* 1993; Cosyns *et al.* 1994). Experimental models of AAN in rodents were developed by our group (Lebeau *et al.* 2005; Baudoux *et al.* 2012). These experimental models recapitulate the structural and functional impairments of renal tissue as observed in humans (Nortier *et al.* 1997; Lebeau *et al.* 2005), including increased oxidative stress, prominent collagen deposits, increased transforming growth factor- β expression and impaired tubular regeneration (Pozdzik *et al.* 2008a), as well as a massive inflammatory cell infiltration (Pozdzik *et al.* 2008b). Interestingly, it has been demonstrated that experimental AAN shows a biphasic evolution of injury, with an early phase (3–10 days) characterized by direct signs of acute kidney injury (AKI), followed by a progressive chronic phase (after 14 days) of interstitial fibrosis and tubular atrophy (Lebeau *et al.* 2005; Pozdzik *et al.* 2008b). Early AKI episodes are characterized by rapid structural and functional alterations of the proximal tubular cells along with increased oxidative stress and impairment of renal function (Lebeau *et al.* 2005; Pozdzik *et al.* 2008a). Therefore, defects in tubular repair, sustained oxidative stress and hypoxia may all contribute to the development of a chronic injury.

Nitric oxide (NO) has been extensively studied and is known to be a key regulator in several physiological processes. In the kidney, NO is involved in the regulation of renal blood flow (Moncada, 1990). It also maintains renal structural integrity (Mount & Power, 2006). Therefore, it has been hypothesized that reduced NO bioavailability

might play a role in the pathogenesis of kidney injury. In previous studies, decreased NO bioavailability was reported in experimental *in vitro* and *in vivo* models of AAN (Wen *et al.* 2008; Liu *et al.* 2011; Tsai *et al.* 2014), and reduced NO production has been linked to sustained hypoxia and ischaemic insult (Wen *et al.* 2008). Furthermore, in addition, the NO precursor L-arginine (L-Arg) has beneficial effects on renal function. L-Arginine has been shown to improve renal NO bioavailability and to limit kidney damage in several pathologies (Schneider *et al.* 2003; Rajapakse *et al.* 2008; Rajapakse & Mattson, 2013). Therefore, in the present study, we hypothesized that NO bioavailability would be reduced during the acute phase of AAN and that L-Arg supplementation would restore its bioavailability, resulting in the protection of tubular integrity and renal function in a model of AAN-induced AKI.

Methods

Experimental protocols

The study conformed to the guiding principles of the American Physiological Society in the care and use of animals and was approved by the Animal Ethics Committee of the University of Namur. Experiments were performed on 8-week-old C57Bl/6 J male mice (Elevage Janvier, Le Genest Saint-Isle, France). Weight-matched mice were randomly assigned to four groups subjected to daily i.p. injection of either sterile saline solution (control) or AA [2.5 mg (kg body weight)⁻¹; Applichem, Darmstadt, Germany] for 4 days. The dose of AA was chosen based on preliminary studies performed in our laboratory (Baudoux *et al.* 2012; Inès Jadot, unpublished data). To determine whether AA-induced renal injuries were related to a reduction in NO, drinking water was supplemented with L-Arg (5%; Sigma-Aldrich, USA) 7 days before the start of the i.p. injection protocol and continued until the end of the experimental protocol. The estimated dose of L-Arg per mouse was about 300 mg (24 h)⁻¹ (Maxwell *et al.* 2001; Alam *et al.* 2013). Mice in the Ctl group ($n = 8$) received daily i.p. injections of sterile saline solution. Mice in the Ctl+L-Arg group ($n = 8$) received daily i.p. injections of sterile saline solution; in addition, these mice were treated with L-Arg administered orally in drinking water. Mice in

the AA group ($n = 8$) received daily I.P. injections of AA solution at $2.5 \text{ mg (kg body weight)}^{-1}$ for 4 days. Mice in the AA+L-Arg group ($n = 8$) received daily I.P. injections of AA solution at $2.5 \text{ mg (kg body weight)}^{-1}$ for 4 days; these mice were also treated with L-Arg administered orally in drinking water.

Body weights (BW) were measured daily in order to adjust the drug dosage. Relative increase of BW was calculated as follows: $[(\text{BW at day 5} - \text{BW at day 1})/(\text{BW at day 1})] \times 100$, where BW at day 1 corresponded to the BW on the first day of AA treatment and BW at day 5 corresponded to the BW at the end of the experiment. Mice were killed by intracardiac puncture and therefore exsanguination on day 5, after a 24 h period in metabolic cages to collect urine. Blood samples were collected and centrifuged at 1600 g for 20 min at 4°C . Plasma was collected and stored at -80°C until use. Immediately after intracardiac puncture, kidneys were excised and subsequently processed for further analysis. Portions of kidneys were snap-frozen in liquid nitrogen for RNA and protein isolation. An additional portion of kidney was fixed in Duboscq–Brasil solution for histological analysis.

Biochemical evaluation of urinary and plasma markers

Plasma and urinary creatinine concentrations were determined by high-performance liquid chromatography (Spherisorb5- μm SCX column, $4.0 \times 250 \text{ mm}$; Waters, Milford, MA, USA). Urinary albumin concentrations were measured using a mouse Albuwell ELISA kit (Exocell, Philadelphia, PA, USA). Total proteinuria was quantified by the Bradford binding assay as previously described (Debelle *et al.* 2002). Urinary excretion of the lysosomal enzyme *N*-acetyl- β -D-glucosaminidase was measured by a colorimetric assay (Roche Diagnostics, Basel, Switzerland), following the manufacturer's protocol (Lebeau *et al.* 2005). As an index of oxidative stress, urine and plasma samples were also analysed for hydrogen peroxide by Amplex red assay (Invitrogen, Carlsbad, CA, USA), following the manufacturer's protocol. Urinary glucose concentrations were also determined (OneTouchVita; LifeScan, Milpitas, CA, USA). All urinary markers were factored by creatinine to obviate any losses in urine collection.

Determination of nitrite/nitrate concentration in urine

Urine samples were diluted 1:100 before performing a nitrate/nitrite colorimetric assay (Cayman Chemical Company, Ann Arbor, MI, USA). This detection kit is based on the Griess method. Briefly, the measurement of total nitrite concentration is performed in a two-step

process: first, nitrate in the urine sample is converted enzymatically to nitrite; and second, nitrite is converted into a deep purple azo compound by the Griess reagents. Absorbance was measured with a spectrophotometer (Versa max micro plate reader; Molecular Devices, Silicon Valley, CA, USA) at 540 nm.

Determination of cyclic guanosine monophosphate (cGMP) concentration in urine

Urine samples were diluted 1:1000 before analysis by cGMP colorimetric assay (Cayman Chemical Company), following the manufacturer's procedures.

Renal tissue superoxide dismutase (SOD) measurement

Tissues samples were homogenized in cold Hepes buffer (Sigma-Aldrich, USA). Tissues were then centrifuged at 1500g for 5 min at 4°C . Supernatants were collected and were analysed by the superoxide dismutase assay kit according to the manufacturer's protocol (Sanbio BV, Uden, The Netherlands).

Osmolarity and Na^+ measurements

Urine osmolarity was measured from freezing point depression using a micro-osmometer (model 210 micro-osmometer; Fiske, Norwood, MA, USA). Plasma sodium (P_{Na}) and urinary sodium concentrations (U_{Na}) were measured using flame photometry (IL943; Instrumentation Laboratories, Lexington, KY, USA).

Semi-quantitative assessment of histopathological alterations

Paraffin-embedded kidney sections were stained with periodic acid–Schiff, hemalun and Luxol Fast Blue for quantification of TI injury, as reported previously (Declèves *et al.* 2006). The degree of tissue injury was assessed on a semi-quantitative basis by means of a double-blind analysis. Each paraffin section was scanned at $\times 400$ magnification, and 10 consecutive fields in renal tissue were analysed. The scoring system was defined as follows: 0, no departure from normal morphology; 1, abnormal large water-filled vacuoles (hydropic degeneration), focal interruptions of brush border or focal cell necrosis; 2, one tubular section containing necrotic or atrophic cells; 3, two to five necrotic or atrophic tubular sections; and 4, more than five necrotic or atrophic tubular sections.

Table 1. Primer sequences

Gene	Direction	Primer sequence (5'–3')
eNOS	Forward	AACCATTCTGTATGGCTCTGAGAC
	Reverse	CTCTAGGGACACCACATCATACTC
iNOS	Forward	CAGCTGGGCTGTACAAACCTT
	Reverse	ATGTGATGTTTGCTTCGGACA
MCP-1	Forward	CTTCTGGGCTGCTGTTCA
	Reverse	CCAGCCTACTCATTGGGATCA
Nox1	Forward	TCCTTCGCTTTTATCGCTCC
	Reverse	TCGCTTCTCATCTGCAATTC
Nox2	Forward	TCCTATGTTCTGTACCTTTGTG
	Reverse	GTCCACCTCCATCTTGAATC
Nox4	Forward	TCCAAGCTCATTTCCACAG
	Reverse	CGGAGTTCATTACATCAGAGG
18S	Forward	CGCCGCTAGAGGTGAAATTCT
	Reverse	CGAACCTCCGACTTTCGTTCT

Immunohistochemistry

Immunostaining of macrophages (Abcam, Cambridge, UK) was performed on paraffin-embedded kidney sections (Declèves *et al.* 2006). Briefly, after dewaxing and rehydration, a microwave pretreatment in citrate buffer (pH 6.2) was performed to unmask antigens in the renal tissue. Tissue sections were then incubated for 1 h with primary antibodies, as follows: anti-macrophage (rat anti-mouse F4/80 antibody, ab56297, 1/50; Abcam, UK) or a specific apoptosis marker, anti-cleaved caspase 3 (rabbit anti-mouse antibody, #9662, 1/200; Cell Signaling, BIOKE, Leiden, The Netherlands). After rinsing in PBS, slides were exposed for 30 min to the appropriate secondary antibody. Finally, kidney sections were incubated with ABC complex (Vector Laboratories, Peterborough, UK) for 30 min, and bound peroxidase activity was detected with the DAB kit (DAKO, Heverlee, Belgium). Counterstaining was performed with hemalun and Luxol Fast Blue.

Cell counts

The frequency of F4/80-positive cells in the interstitial spaces and the frequency of activated caspase 3-positive cells were evaluated by semi-quantitative analysis as described previously (Declèves *et al.* 2006). The distribution of positive cells was assessed on one section per experimental animal. For each section, 10 square fields (0.084 mm² per field) were observed in the cortex and in the outer medulla at $\times 400$ magnification. Quantification was performed by means of a double-blind analysis.

Quantitative real-time PCR

Frozen kidney samples (-80°C) were homogenized and total RNA was extracted. Quantification of mRNA was

performed using two-step real-time reverse-transcriptase-PCR (LightCycler; Roche Diagnostics). Real-time PCR was performed on kidney using the primers for eNOS, iNOS, MCP-1, *Nox1*, *Nox2* and *Nox4*, with *18S* as a housekeeping gene, designed by and purchased from Eurogentec (Seraing, Belgium; Table 1). Relative gene expression was calculated using the $2^{-\Delta\Delta C_t}$ method.

Statistics

Results are presented as mean values \pm SEM. The level for statistical significance was defined as $P < 0.05$. One-way ANOVA was applied for multiple intergroup comparisons followed by the Newman–Keuls *post hoc* test for multiple comparisons. When assessing the degree of tissue necrosis, non-parametric Kruskal–Wallis one-way ANOVA followed by Dunn's multiple comparison test were applied to identify significant differences between groups. Analyses were carried out using GraphPad Software Inc, La Jolla, CA, USA.

Results

General observations in control mice or mice after AA intoxication with or without L-Arginine supplementation

As illustrated in Table 2, the relative increase in BW observed both in Ctl and Ctl+L-Arg mice was significantly lower in AA-treated mice. L-Arg supplementation did not ameliorate this change. In contrast, there was no significant difference in kidney weight between groups. No differences were observed regarding food and water intake.

Table 2. General observations in Ctl, Ctl+L-Arg, AA and AA+L-Arg groups of mice

Characteristic	Ctl	Ctl+L-Arg	AA	AA+L-Arg
Relative increase of body weight (%)	7.65 ± 0.89	10.12 ± 1.39	2.21 ± 0.68*†	2.21 ± 1.45*†
Kidney weight (mg)	156.9 ± 6.4	163.7 ± 6.4	168.3 ± 4.0	171.1 ± 4.7
Food intake [g (24 h) ⁻¹]	3.90 ± 0.19	3.98 ± 0.18	3.71 ± 0.13	3.43 ± 0.14
Water intake [ml (24 h) ⁻¹]	5.69 ± 0.53	5.91 ± 0.55	5.94 ± 0.34	5.42 ± 0.32

Abbreviations: AA, aristolochic acid; and Ctl, control. Values are means ± SEM. $n = 8$ in each group. Statistical analyses were performed by one-way ANOVA followed by Newman–Keuls test. * $P \leq 0.05$ versus Ctl mice; and † $P \leq 0.05$ versus Ctl+L-Arg mice.

L-Arginine supplementation prevents the AA-induced decrease in NO bioavailability

In order to determine whether L-Arg supplementation could affect NO bioavailability, we measured urinary NO metabolite (NO_x) concentrations at day 5 in control mice and in mice after AA intoxication with or without L-Arg supplementation (Fig. 1A). As illustrated, urinary NO_x concentrations were significantly lower in AA-treated mice {1.64 ± 0.26 versus 2.49 ± 0.13 and 3.01 ± 0.28 μmol [mg creatinine (Cre)]⁻¹ in Ctl and Ctl+L-Arg groups, respectively}, whereas L-Arg supplementation completely normalized this change [2.71 ± 0.20 μmol (mg Cre)⁻¹].

The most well-known target of NO is guanylate cyclase, which is responsible for the synthesis of cGMP. Owing to its connection with NO, cGMP is frequently used to evaluate the rate of NO production (Csonka *et al.* 2015). In this case, urinary cGMP concentrations decreased significantly with AA treatment, and L-Arg supplementation significantly attenuated this decrease (Fig. 1B).

Table 3 shows that mRNA levels for *eNOS* and *iNOS* measured in renal tissue did not differ between groups. Treatment with L-Arg in AA-injected mice resulted in a slight trend towards reduced *iNOS* mRNA levels, but this result did not reach statistical significance.

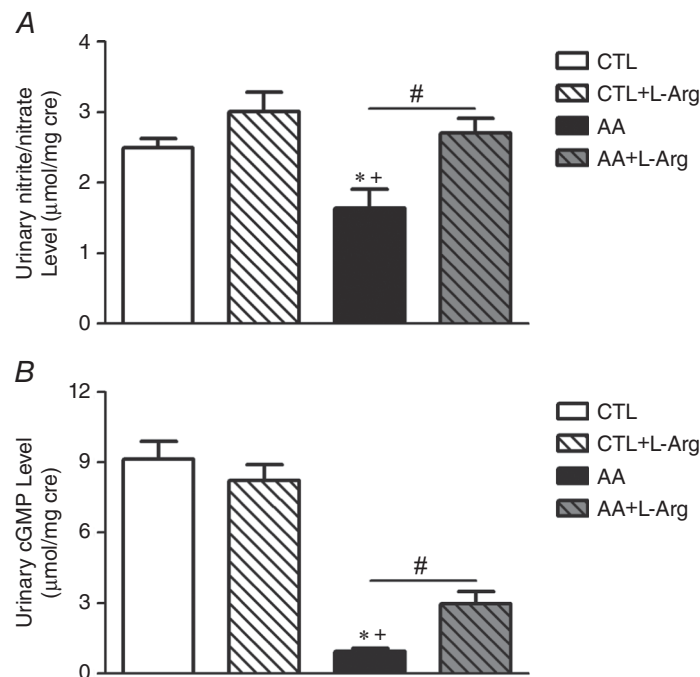


Figure 1. L-Arginine (L-Arg) supplementation prevents aristolochic acid (AA)-induced decreased NO bioavailability

Quantitative urinary nitrite/nitrate (NO_x) concentrations, A, and urinary cGMP concentrations, B, in control (Ctl), Ctl+L-Arg, AA and AA+L-Arg groups of mice. Values are means ± SEM. $n = 8$ in each group. Statistical analyses were performed by one-way ANOVA followed by Newman–Keuls test. * $P \leq 0.05$ versus Ctl mice; + $P \leq 0.05$ versus Ctl+L-Arg mice; and # $P \leq 0.05$ versus AA-treated mice.

Table 3. Effect of L-Arg supplementation on renal eNOS and iNOS gene expression in Ctl, Ctl+L-Arg, AA and AA+L-Arg groups of mice

Gene	Ctl	Ctl+L-Arg	AA	AA+L-Arg
eNOS	1.00 ± 0.32	1.36 ± 0.51	1.50 ± 0.33	1.57 ± 0.67
iNOS	1.00 ± 0.19	1.01 ± 0.30	1.08 ± 0.21	0.52 ± 0.11

Abbreviations: AA, aristolochic acid; Ctl, control; eNOS, endothelial nitric oxide synthase; iNOS, inducible nitric oxide synthase. Values are means ± SEM. $n = 8$ in each group. Statistical analyses were performed by one-way ANOVA followed by Newman–Keuls test. No significant differences were found.

Table 4. Effect of L-Arg supplementation on renal function in Ctl, Ctl+L-Arg, AA and AA+L-Arg groups of mice

Parameter	Ctl	Ctl+L-Arg	AA	AA+L-Arg
Plasma creatinine (mg dl ⁻¹)	0.14 ± 0.02	0.11 ± 0.02	0.57 ± 0.04*†	0.42 ± 0.03*†‡
Creatinine clearance (ml min ⁻¹)	0.42 ± 0.06	0.34 ± 0.04	0.11 ± 0.02*†	0.20 ± 0.02*†‡
Diuresis [ml (24 h) ⁻¹]	1.14 ± 0.20	1.39 ± 0.17	2.22 ± 0.14*†	1.53 ± 0.20‡
Fractional excretion of sodium (%)	0.31 ± 0.03	0.32 ± 0.03	1.43 ± 0.27*†	0.83 ± 0.07‡
Osmolality (mosmol kg ⁻¹)	5704 ± 604	5629 ± 565	3505 ± 464*†	5221 ± 510‡
Urine glucose [mg (24 h) ⁻¹]	1.56 ± 0.21	1.35 ± 0.11	97.75 ± 6.63*†	60.70 ± 11.22*†‡

Abbreviations: AA, aristolochic acid; and Ctl, control. Values are means ± SEM. $n = 8$ in each group. Statistical analyses were performed by one-way ANOVA followed by Newman–Keuls test. * $P \leq 0.05$ versus Ctl mice; † $P \leq 0.05$ versus Ctl+L-Arg mice; and ‡ $P \leq 0.05$ versus AA-treated mice.

L-Arginine supplementation ameliorates AA-induced impairment of renal function

As shown in Table 4, an acute kidney injury, reflected by a significant increase in plasma creatinine concentration, was established in AA-treated mice at day 5 compared with the control groups. In the AA+L-Arg group, although plasma creatinine concentrations were still higher than in the control group, L-Arg supplementation significantly attenuated this change ($P < 0.05$). In order to confirm this result, creatinine clearance values were also determined. Aristolochic acid (AA)-treated mice showed a significant decrease in creatinine clearance, which was significantly ameliorated by L-Arg treatment ($P < 0.05$).

Urine volume measurements revealed that AA-treated mice had a clear and significant increase compared with the control groups, demonstrating that AA intoxication induced polyuria. This rise was prevented in mice supplemented with L-Arg. In order to characterize renal function further, and tubular function in particular, we evaluated renal sodium handling by measuring fractional excreted sodium. Samples from AA-treated mice showed significantly increased fractional excreted sodium, suggesting increased levels of wasted salt associated with AA intoxication. This change was prevented by L-Arg supplementation. In addition, urine osmolality significantly decreased and urine glucose concentrations significantly increased in AA-treated mice, and these changes were alleviated by L-Arg supplementation ($P < 0.05$).

We also investigated whether L-Arg supplementation affected urinary protein concentrations and albuminuria, two other markers of renal damage. AA-treated mice exhibited significantly increased proteinuria and albuminuria, which were significantly attenuated by L-Arg supplementation ($P < 0.05$; Fig. 2A and B). Moreover, urinary excretion of the lysosomal enzyme *N*-acetyl- β -D-glucosaminidase, a marker of tubular damage (Lebeau *et al.* 2005), was significantly increased in AA-treated mice (Fig. 2C), reflecting structural impairment of proximal tubular epithelial cells. This change was also prevented by L-Arg supplementation.

Effect of L-Arginine supplementation on AA-induced tissue injury

Conventional microscopy using periodic acid–Schiff staining revealed morphological alterations in renal tissue after AA intoxication (Fig. 3). As illustrated in Fig. 3A–F, control mice did not show any histological abnormalities, i.e. tubular structures were preserved and tubular epithelial cells were normal. However, patchy zones of necrotic proximal tubular epithelial cells (dotted ovals) were observed in AA-treated mice in the outer stripe of the outer medulla (OSOM), with some extension to the cortex. Necrotic cells (NT) and cellular fragments (arrows) were also found in the lumen of the proximal tubules (Fig. 3G–I). In AA+L-Arg-treated mice, tubular damage was significantly reduced. A limited number of

necrotic tubules were observed within a better-preserved tubular structure (Fig. 3J–L). The quantitative score of tubular injury (Fig. 3M) revealed a tubular necrosis score significantly higher in AA-treated mice than in control mice, and L-Arg supplementation significantly reduced the necrosis score compared with AA groups ($P < 0.05$). Regarding glomerular histology, no major microscopic damage was observed. Therefore, histological AAN injuries are mostly located in proximal tubular epithelial cells with microscopically well-preserved glomeruli.

L-Arginine supplementation prevents tubular cell apoptosis in AA-induced tissue injury

Tubular cell apoptosis was demonstrated by the expression of activated caspase 3. As illustrated in Fig. 4, a significant increase in tubular epithelial cell apoptosis was detected in AA-treated mice as reflected by the increase in activated caspase 3 nuclear expression (Fig. 4A, C and E). This increase was prevented by L-Arg supplementation (Fig. 4B, D and E).

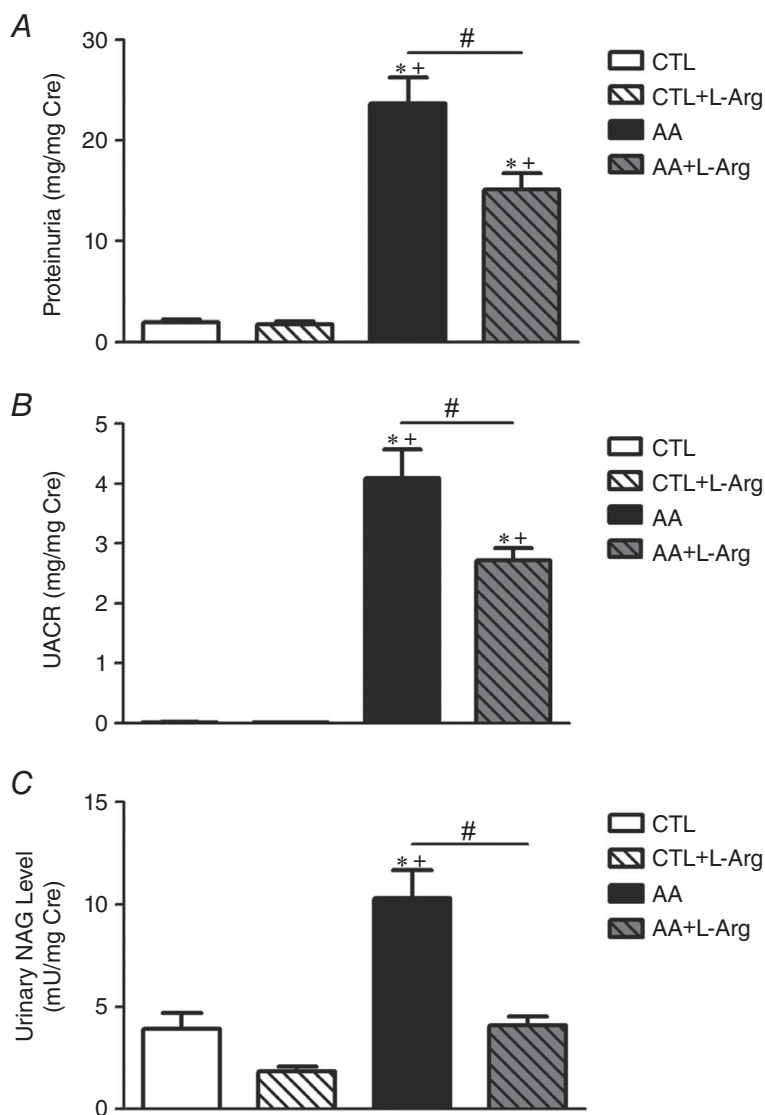


Figure 2. Effect of L-Arg supplementation on urine protein, albumin levels and N-acetyl- β -d-glucosaminidase (NAG) enzymuria level in Ctl, Ctl+L-Arg, AA and AA+L-Arg groups of mice. **A**, quantitative urine total protein levels. **B**, quantitative urine albumin/creatinine ratios (UACR). **C**, quantitative urine NAG enzymuria levels in Ctl, Ctl+L-Arg, AA and AA+L-Arg groups of mice. Values are means \pm SEM. $n = 8$ in each group. Statistical analyses were performed by one-way ANOVA followed by Newman–Keuls test. * $P \leq 0.05$ versus Ctl mice; + $P \leq 0.05$ versus Ctl+L-Arg mice; and # $P \leq 0.05$ versus AA-treated mice.

Effect of L-Arginine supplementation on AA-induced inflammatory markers

To determine the effect of L-Arg supplementation on renal inflammation, monocyte chemoattractant protein-1 (MCP-1) mRNA levels and macrophage infiltration were investigated. As observed in Fig. 5, the mRNA levels

of the early pro-inflammatory cytokine, MCP-1, were significantly increased in AA-treated mice. This was prevented by L-Arg supplementation ($P < 0.05$) (Fig. 5A). Moreover, although macrophage infiltration tended to be higher in the AA group, this change did not reach statistical significance. A similar result was observed in the AA+L-Arg group (Fig. 5B–F).

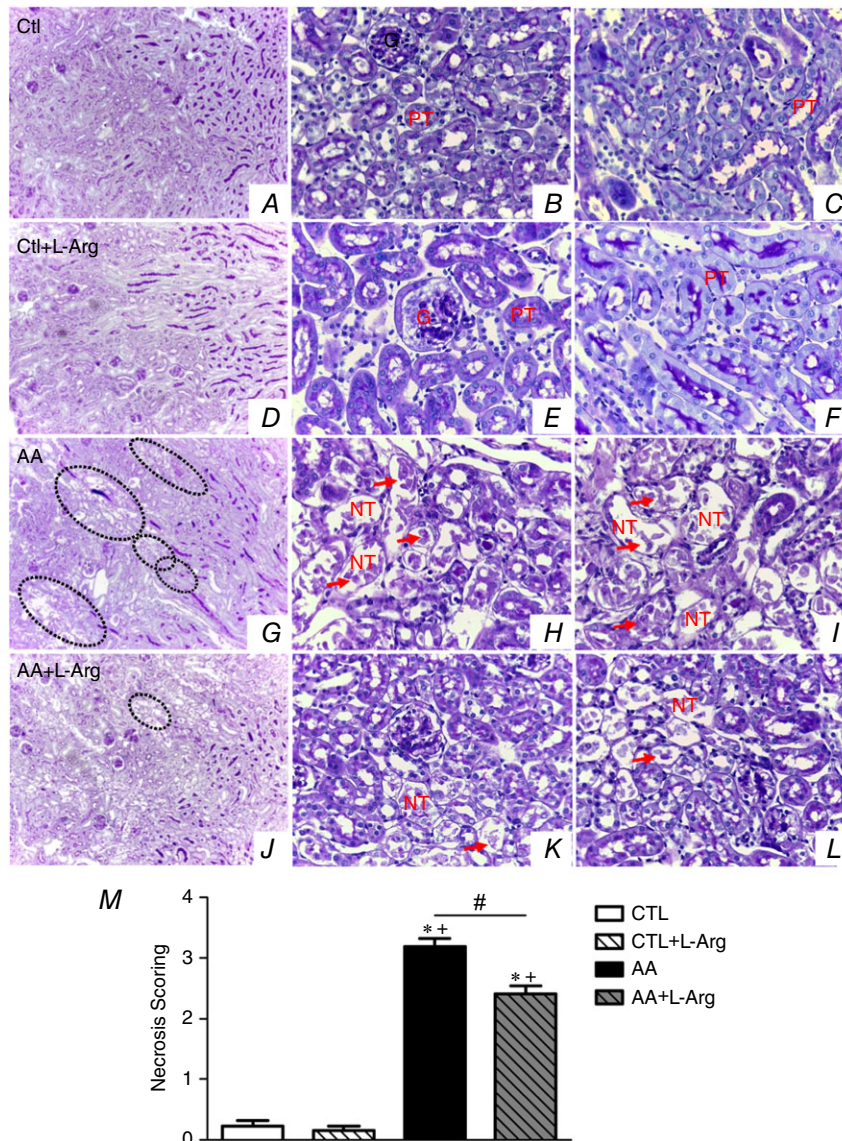


Figure 3. Effect of L-Arg supplementation on AA-induced tissue injury

Effects of L-Arg supplementation on renal tissue injury in Ctl, Ctl+L-Arg, AA and AA+L-Arg groups of mice. Representative photomicrographs ($\times 200$ magnification in A, D, G and J; and $\times 400$ magnification in B, C, E, F, H, I, K and L) illustrating renal tissue injury with periodic acid–Schiff staining in Ctl (A–C), Ctl+L-Arg (D–F), AA (G–I) and AA+L-Arg groups of mice (J–L). M, Semi-quantitative analysis of tubular injury at day 5 in Ctl, Ctl+L-Arg, AA, and AA+L-Arg groups of mice. Values are means \pm SEM. $n = 8$ in each group. Statistical analyses were performed by non-parametric Kruskal–Wallis one-way ANOVA followed by Dunn's multiple comparison test. * $P \leq 0.05$ versus Ctl mice; + $P < 0.05$ versus Ctl+L-Arg mice; and # $P \leq 0.05$ versus AA mice. Abbreviations: G, glomerulus; NT, necrotic tubule; and PT, proximal tubule. Arrows indicate cellular fragments in the lumen of the necrotic proximal tubules.

Effect of L-Arginine supplementation on AA-induced oxidative stress and antioxidant SOD activity

In order to evaluate the potential effect of L-Arg supplementation on AA-induced oxidative stress, NADPH oxidases, known to be a major source of reactive oxygen species (ROS) in kidney, were investigated at the mRNA level. Table 5 illustrates the renal mRNA levels for Nox1, Nox2 and Nox4. Nox1 and Nox4 mRNA levels were unchanged in all groups. However, Nox2 mRNA levels were significantly higher in AA-treated mice, and this increase was prevented by L-Arg supplementation. Given that Nox2 is a major source of reactive oxygen species, we determined urinary and plasma hydrogen peroxide concentrations as the stable product of ROS production (Fig. 6A

and B). Urinary hydrogen peroxide concentrations were significantly higher after AA intoxication and were reduced with L-Arg supplementation ($P < 0.05$; Fig. 6A). In plasma, the increase of hydrogen peroxide in AA-treated mice was significantly attenuated in the AA+L-Arg-treated group (Fig. 6B). Therefore, the increase in urinary hydrogen peroxide is likely to be contributed to by both systemic and renal production of hydrogen peroxide, and these are improved by L-Arg. Finally, total SOD activity was determined in renal tissue homogenates (Fig. 6C). As illustrated in Fig. 6C, the SOD concentration was unchanged in AA-treated mice. However, total SOD activity showed a significant increase with L-Arg supplementation ($P < 0.05$).

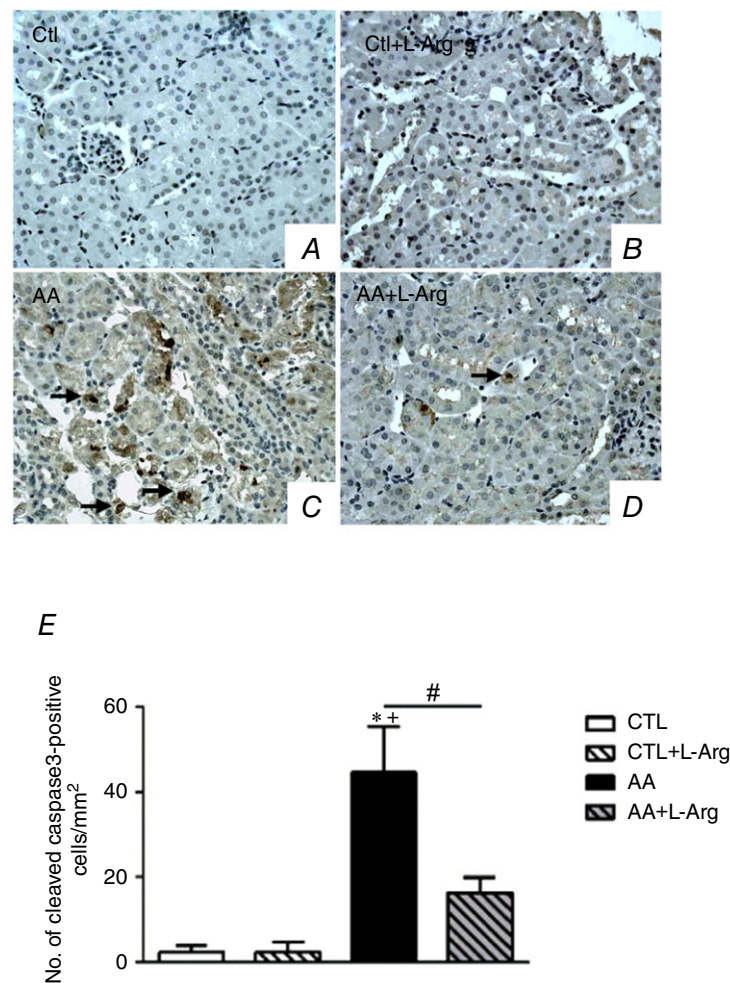


Figure 4. Effect of L-Arg supplementation on apoptosis

Effects of L-Arg supplementation on cell apoptosis in Ctl, Ctl+L-Arg, AA and AA+L-Arg groups of mice. Representative photomicrographs ($\times 400$ magnification, A–D) illustrating cleaved caspase 3-positive staining in Ctl (A), Ctl+L-Arg (B), AA (C) and AA+L-Arg (D) groups of mice. E, quantitative analysis of cleaved caspase 3-positive staining at day 5. Values are means \pm SEM. $n = 8$ in each group. Statistical analyses were performed by one-way ANOVA followed by Newman–Keuls test. * $P \leq 0.05$ versus Ctl mice; + $P < 0.05$ versus Ctl+L-Arg mice; and # $P \leq 0.05$ versus AA mice.

Discussion

Human AAN is a good example of a progressive TI nephritis that can lead to fibrosis and end-stage renal disease. Our group has unravelled several features of this

disease using specific rodent models (Lebeau *et al.* 2005; Pozdzik *et al.* 2008*a,b*; Baudoux *et al.* 2012). In particular, we have identified the presence of two interconnected phases: an acute phase and a chronic phase. The acute phase consists of an episode of AKI characterized by

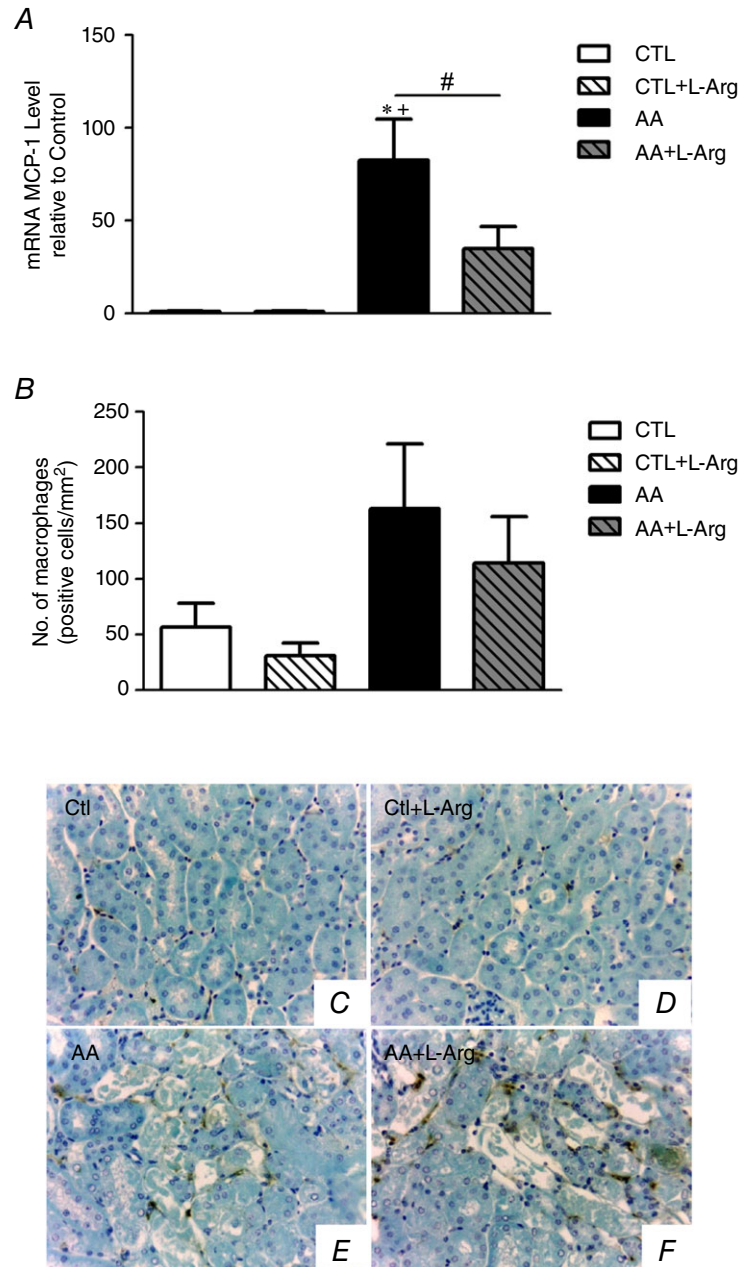


Figure 5. Effect of L-Arg supplementation on AA-induced inflammatory markers

A, quantitative real-time PCR for *MCP-1* mRNA expression was performed with kidney tissue from Ctl, Ctl+L-Arg, AA and AA+L-Arg groups of mice normalized against *18S*. **B**, quantitative analysis of number of F4/80-positive cells in renal tissue in Ctl, Ctl+L-Arg, AA and AA+L-Arg groups of mice. **C–F**, representative photomicrographs ($\times 400$ magnification) of macrophage staining in Ctl (**C**), Ctl+L-Arg (**D**), AA (**E**) and AA+L-Arg groups of mice (**F**). Values are means \pm SEM. $n = 8$ in each group. Statistical analyses were performed by one-way ANOVA followed by Newman–Keuls test. $*P \leq 0.05$ versus Ctl mice; $+P < 0.05$ versus Ctl+L-Arg mice; and $\#P \leq 0.05$ versus AA mice.

Table 5. Effect of L-Arg supplementation on renal *Nox1*, *Nox2* and *Nox4* gene expression in Ctl, Ctl+L-Arg, AA and AA+L-Arg groups of mice

Gene	Ctl	Ctl+L-Arg	AA	AA+L-Arg
<i>Nox1</i>	1.00 ± 0.30	0.91 ± 0.33	1.27 ± 0.18	1.45 ± 0.41
<i>Nox2</i>	1.00 ± 0.59	0.64 ± 0.16	4.35 ± 1.55*†	0.81 ± 0.19‡
<i>Nox4</i>	1.00 ± 0.18	0.83 ± 0.28	0.33 ± 0.08	0.81 ± 0.25

Abbreviations: AA, aristolochic acid; and Ctl, control. Values are means ± SEM. $n = 8$ in each group. Statistical analyses were performed by one-way ANOVA followed by Newman–Keuls test. * $P \leq 0.05$ versus Ctl mice; † $P < 0.05$ versus Ctl+L-Arg mice; and ‡ $P \leq 0.05$ versus AA mice.

increased plasma creatinine concentrations and tubular necrosis, whereas the chronic phase features interstitial fibrosis and tubular atrophy (Lebeau *et al.* 2005). Nowadays, there is strong evidence that an episode of AKI can lead to subsequent development of a chronic injury (Lai *et al.* 2012; Zager *et al.* 2013; Harel *et al.* 2014; Tanaka *et al.* 2014). A better understanding of the mechanisms that underlie the AAN-induced AKI phase is necessary to develop therapeutic strategies.

In this study, we demonstrated that NO is involved in the AKI phase of AA-induced nephropathy. Nitric oxide is a paracrine factor involved in physiological and pathological conditions. Synthesis of NO occurs through activation of NO synthases (NOSs). In the kidney, NO is known to be involved in the regulation of vascular resistance, glomerular filtration rate, water and sodium excretion, and in the maintenance of renal structural integrity (Mount & Power, 2006; Kwon *et al.* 2009). In addition, NO has beneficial or deleterious effects depending on its concentration, duration of release and site of production (Goligorsky *et al.* 2002; Kwon *et al.* 2009). Previous investigations have reported a reduction of NO production associated with AA treatment in glomerular mesangial cells or macrophage cells (Liu *et al.* 2011; Tsai *et al.* 2014). In another study using an experimental AAN model in rats, attenuation of NO production was demonstrated along with increased endothelin-1 and hypoxia-inducible factor-1 α expression and decreased vascular endothelial growth factor (Wen *et al.* 2008). These results suggest that pathogenesis of AAN is associated with an ischaemic insult to the kidney.

In our study, decreased NO bioavailability, as demonstrated by reductions in NO₂ and NO₃ metabolites as well as cGMP concentrations, was found in AA-treated mice. Our data show that L-Arg supplementation increased NO production which, in turn, improved renal function and tubular integrity. Overall renal function (creatininaemia, polyuria, proteinuria and *N*-acetyl- β -D-glucosaminidase enzymuria) and renal structural injury (tubular necrosis and tubular cell apoptosis) were prevented by L-Arg treatment. Moreover, acute AA tubulotoxicity resulted in increases in fractional

sodium excretion and urine glucose concentrations, reflecting a defect in tubular function (Waz *et al.* 1998; Voisin *et al.* 2014). These changes were also prevented by L-Arg treatment.

Even more interestingly, our data show that, in parallel with the change in NO production, there were significant increases in *Nox2* expression and hydrogen peroxide concentrations, both markers of oxidative stress. The NADPH oxidases (NOXs), especially *Nox1*, *Nox2* and *Nox4*, are widely expressed in the kidney and are well known to be a major source of ROS (Sedeek *et al.* 2013). In our study, although the expression levels of *Nox1* and *Nox4* were unchanged, we found a significant increase in *Nox2* expression in AA-treated mice. This increase was prevented by L-Arg treatment. Several investigations have implicated NOX2 in renal vascular dysfunction (Carlstrom *et al.* 2009; Schlüter *et al.* 2010). NOX2 has been reported to contribute to the control of renal perfusion, especially in contractile response i.e. modulation of the vascular tone of arterioles via contractile elements, and this was partly due to its inhibitory action on NO bioavailability (Carlstrom *et al.* 2009). NOX2 is indeed a major source of ROS that were demonstrated to scavenge NO, reducing NO bioavailability (Ren *et al.* 2002). In physiological conditions, NO maintains endothelial function because of its vasoactive effects, promoting increased renal blood flow, blunting tubuloglomerular feedback and scavenging low ROS concentrations. Here, the increase in NO bioavailability brought about by L-Arg supplementation decreased *Nox2* expression and this, in turn, attenuated the NOX2-induced oxidative stress.

In parallel to an increase of *Nox2* mRNA levels, we also observed a significant increase of hydrogen peroxide in both urine and plasma samples from AA-treated mice, reinforcing the hypothesis that NO availability is limited by ROS production. However, our data indicate that maintaining NO production by pharmacological manipulation was beneficial for reducing ROS production. This, in turn, contributes to amelioration of overall renal and tubular function in AAN-induced AKI.

Finally, even though AA intoxication was not associated with decreased SOD concentrations, there was evidence

of higher SOD concentrations after L-Arg treatment. This result, in parallel with the marked increase in NO production in L-Arg-treated mice, might suggest that NO is beneficial in increasing renal capacity to neutralize oxidative bursts.

In summary, we have shown that our old friend, NO, plays a major role in the acute phase of the AAN model. Here, rapid evolution of AKI was associated with a

significant reduction in NO bioavailability, renal injury and tubular dysfunction. Increased NO bioavailability significantly reduced these changes. This was associated with significant reductions in *Nox2* expression and ROS production. These data may prove helpful for guiding the design of more specific therapeutic approaches in order to preserve renal function and renal structures in AA-induced AKI.

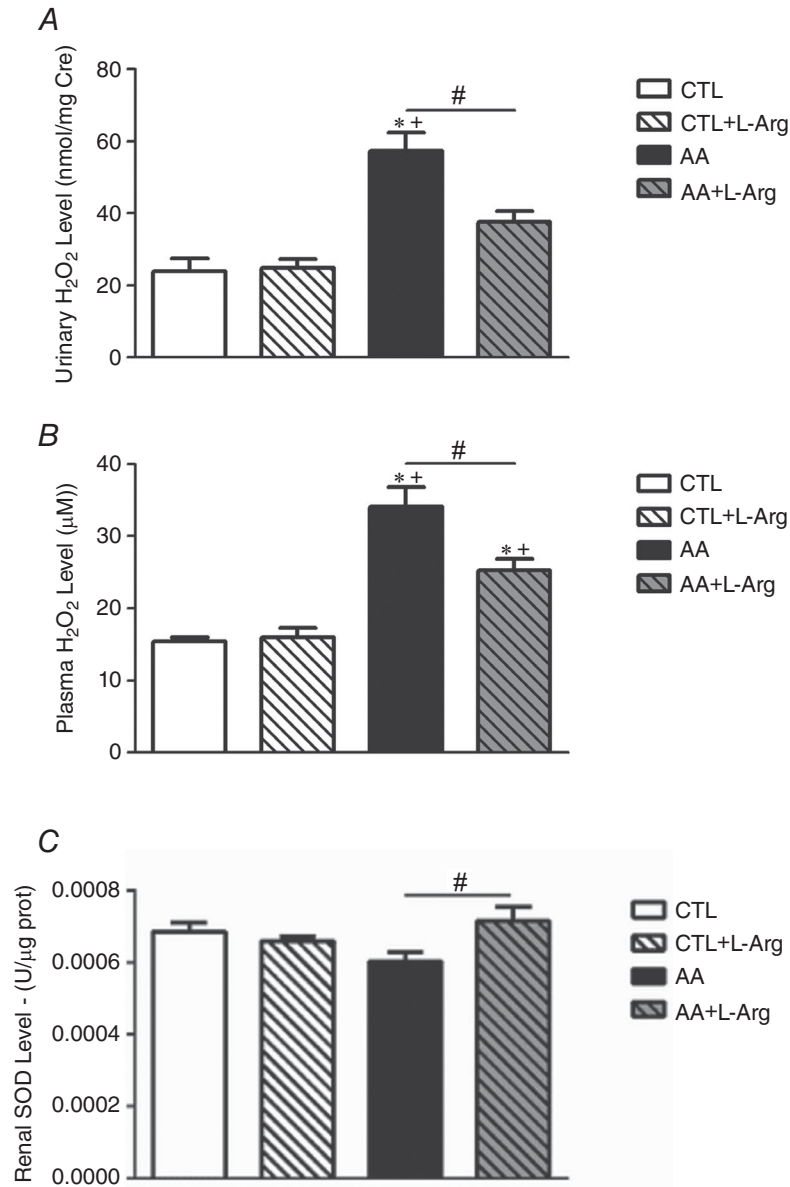


Figure 6. Effect of L-Arg supplementation on AA-induced oxidative stress and antioxidant superoxide dismutase (SOD) activity

Quantitative urine hydrogen peroxide (H₂O₂)/creatinine concentration in Ctl, Ctl+L-Arg, AA and AA+L-Arg groups of mice. *B*, quantitative plasma H₂O₂ concentration. *C*, quantitative renal total SOD concentration. Values are means ± SEM. *n* = 8 in each group. Statistical analyses were performed by one-way ANOVA followed by Newman–Keuls test. **P* ≤ 0.05 versus Ctl mice; +*P* < 0.05 versus Ctl+L-Arg mice; and #*P* ≤ 0.05 versus AA mice.

References

- Alam MA, Kauter K, Withers K, Sernia C & Brown L (2013). Chronic L-arginine treatment improves metabolic, cardiovascular and liver complications in diet-induced obesity in rats. *Food Funct* **4**, 83–91.
- Baudoux TE, Pozdzik AA, Arlt VM, De Prez EG, Antoine MH, Quellard N, Goujon JM & Nortier JL (2012). Probenecid prevents acute tubular necrosis in a mouse model of aristolochic acid nephropathy. *Kidney Int* **82**, 1105–1113.
- Carlstrom M, Lai EY, Ma Z, Patzak A, Brown RD & Persson AE (2009). Role of NOX2 in the regulation of afferent arteriole responsiveness. *Am J Physiol Regul Integr Comp Physiol* **296**, R72–R79.
- Cosyns JP, Jadoul M, Squifflet JP, De Plaen JF, Ferluga D & van Ypersele de Strihou C (1994). Chinese herbs nephropathy: a clue to Balkan endemic nephropathy? *Kidney Int* **45**, 1680–1688.
- Csonka C, Pali T, Bencsik P, Gorbe A, Ferdinandy P & Csont T (2015). Measurement of NO in biological samples. *Br J Pharmacol* **172**, 1620–1632.
- Debelle FD, Nortier JL, De Prez EG, Garbar CH, Vienne AR, Salmon IJ, Deschodt-Lanckman MM & Vanherweghem JL (2002). Aristolochic acids induce chronic renal failure with interstitial fibrosis in salt-depleted rats. *J Am Soc Nephrol* **13**, 431–436.
- Debelle FD, Vanherweghem JL & Nortier JL (2008). Aristolochic acid nephropathy: a worldwide problem. *Kidney Int* **74**, 158–169.
- Declèves AE, Caron N, Nonclercq D, Legrand A, Toubeau G, Kramp R & Flamion B (2006). Dynamics of hyaluronan, CD44, and inflammatory cells in the rat kidney after ischemia/reperfusion injury. *Int J Mol Med* **18**, 83–94.
- Goligorsky MS, Brodsky SV & Noiri E (2002). Nitric oxide in acute renal failure: NOS versus NOS. *Kidney Int* **61**, 855–861.
- Grollman AP, Shibutani S, Moriya M, Miller F, Wu L, Moll U, Suzuki N, Fernandes A, Rosenquist T, Medverec Z, Jakovina K, Brdar B, Slade N, Turesky RJ, Goodenough AK, Rieger R, Vukelić M & Jelaković B (2007). Aristolochic acid and the etiology of endemic (Balkan) nephropathy. *Proc Natl Acad Sci USA* **104**, 12129–12134.
- Harel Z, Bell CM, Dixon SN, McArthur E, James MT, Garg AX, Harel S, Silver S & Wald R (2014). Predictors of progression to chronic dialysis in survivors of severe acute kidney injury: a competing risk study. *BMC Nephrol* **15**, 114.
- Kwon O, Hong SM & Ramesh G (2009). Diminished NO generation by injured endothelium and loss of macula densa nNOS may contribute to sustained acute kidney injury after ischemia-reperfusion. *Am J Physiol Renal Physiol* **296**, F25–F33.
- Lai CF, Wu VC, Huang TM, Yeh YC, Wang KC, Han YY, Lin YF, Jhuang YJ, Chao CT, Shiao CC, Tsai PR, Hu FC, Chou NK, Ko WJ & Wu KD (2012). Kidney function decline after a non-dialysis-requiring acute kidney injury is associated with higher long-term mortality in critically ill survivors. *Crit Care* **16**, R123.
- Lebeau C, Debelle FD, Arlt VM, Pozdzik A, De Prez EG, Phillips DH, Deschodt-Lanckman MM, Vanherweghem JL & Nortier JL (2005). Early proximal tubule injury in experimental aristolochic acid nephropathy: functional and histological studies. *Nephrol Dial Transplant* **20**, 2321–2332.
- Liu MC, Lin TH, Wu TS, Yu FY, Lu CC & Liu BH (2011). Aristolochic acid I suppressed iNOS gene expression and NF- κ B activation in stimulated macrophage cells. *Toxicol Lett* **202**, 93–99.
- Maxwell AJ, Ho HV, Le CQ, Lin PS, Bernstein D & Cooke JP (2001). L-Arginine enhances aerobic exercise capacity in association with augmented nitric oxide production. *J Appl Physiol* **90**, 933–938.
- Moncada S (1990). The first Robert Furchgott lecture: from endothelium-dependent relaxation to the L-arginine:NO pathway. *Blood Vessels* **27**, 208–217.
- Mount PF & Power DA (2006). Nitric oxide in the kidney: functions and regulation of synthesis. *Acta Physiol (Oxf)* **187**, 433–446.
- Nortier JL, Deschodt-Lanckman MM, Simon S, Thielemans NO, de Prez EG, Depierreux MF, Tielemans CL, Richard C, Lauwerys RR, Bernard AM & Vanherweghem JL (1997). Proximal tubular injury in Chinese herbs nephropathy: monitoring by neutral endopeptidase enzymuria. *Kidney Int* **51**, 288–293.
- Pozdzik AA, Salmon IJ, Debelle FD, Decaestecker C, Van den Branden C, Verbeelen D, Deschodt-Lanckman MM, Vanherweghem JL & Nortier JL (2008a). Aristolochic acid induces proximal tubule apoptosis and epithelial to mesenchymal transformation. *Kidney Int* **73**, 595–607.
- Pozdzik AA, Salmon IJ, Husson CP, Decaestecker C, Rogier E, Bourgeade MF, Deschodt-Lanckman MM, Vanherweghem JL & Nortier JL (2008b). Patterns of interstitial inflammation during the evolution of renal injury in experimental aristolochic acid nephropathy. *Nephrol Dial Transplant* **23**, 2480–2491.
- Raj L (2008). Nitric oxide and cardiovascular and renal effects. *Osteoarthritis Cartilage* **16** Suppl 2, S21–S26.
- Rajapakse NW, De Miguel C, Das S & Mattson DL (2008). Exogenous L-arginine ameliorates angiotensin II-induced hypertension and renal damage in rats. *Hypertension* **52**, 1084–1090.
- Rajapakse NW & Mattson DL (2013). Role of cellular L-arginine uptake and nitric oxide production on renal blood flow and arterial pressure regulation. *Curr Opin Nephrol Hypertens* **22**, 45–50.
- Ren Y, Carretero OA & Garvin JL (2002). Mechanism by which superoxide potentiates tubuloglomerular feedback. *Hypertension* **39**, 624–628.
- Schlüter T, Zimmermann U, Protzel C, Miede B, Klebingat KJ, Rettig R & Grisk O (2010). Intrarenal artery superoxide is mainly NADPH oxidase-derived and modulates endothelium-dependent dilation in elderly patients. *Cardiovasc Res* **85**, 814–824.
- Schneider R, Raff U, Vornberger N, Schmidt M, Freund R, Reber M, Schramm L, Gambaryan S, Wanner C, Schmidt HH & Galle J (2003). L-Arginine counteracts nitric oxide deficiency and improves the recovery phase of ischemic acute renal failure in rats. *Kidney Int* **64**, 216–225.

- Sedeek M, Nasrallah R, Touyz RM & Hebert RL (2013). NADPH oxidases, reactive oxygen species, and the kidney: friend and foe. *J Am Soc Nephrol* **24**, 1512–1518.
- Tanaka S, Tanaka T & Nangaku M (2014). Hypoxia as a key player in the AKI-to-CKD transition. *Am J Physiol Renal Physiol* **307**, F1187–F1195.
- Tsai KD, Chen W, Wang SH, Hsiao YW, Chi JY, Wu HY, Lee YJ, Wong HY, Tseng MJ & Lin TH (2014). Downregulation of connective tissue growth factor by LPS/IFN- γ -induced nitric oxide is reversed by aristolochic acid treatment in glomerular mesangial cells via STAT-1 α and NF- β B signaling. *Chem Biol Interact* **210**, 86–95.
- Vanherweghem JL, Depierreux M, Tielemans C, Abramowicz D, Dratwa M, Jadoul M, Richard C, Vandervelde D, Verbeelen D, Vanhaelen-Fastre R & Vanhaelen M (1993). Rapidly progressive interstitial renal fibrosis in young women: association with slimming regimen including Chinese herbs. *Lancet* **341**, 387–391.
- Voisin V, Declèves A, Hubert V, Colombaro V, Giordano L, Habsch I, Bouby N, Nonclercq D & Caron N (2014). Protection of Wistar-Furth rats from postischemic acute renal injury: role for nitric oxide and thromboxane? *Clin Exp Pharmacol Physiol* **41**, 911–920.
- Waz WR, Van Liew JB & Feld LG (1998). Nitric oxide metabolism following unilateral renal ischemia/reperfusion injury in rats. *Pediatr Nephrol* **12**, 26–29.
- Wen YJ, Qu L & Li XM (2008). Ischemic injury underlies the pathogenesis of aristolochic acid-induced acute kidney injury. *Transl Res* **152**, 38–46.
- Zager RA, Johnson AC, Andress D & Becker K (2013). Progressive endothelin-1 gene activation initiates chronic/end-stage renal disease following experimental ischemic/reperfusion injury. *Kidney Int* **84**, 703–712.

Additional information

Competing interests

None declared.

Author contributions

N.C., J.N. and A.-E.D. conceived the experiments. I.J., B.M., V.C., V.V. and A.-E.D. performed the experiments. N.C. and J.N. oversaw the experiments that were performed in their respective laboratories. I.J. and A.-E.D. prepared the manuscript. All authors have approved the final version of the manuscript and agree to be accountable for all aspects of the work. All persons designated as authors qualify for authorship, and all those who qualify for authorship are listed.

Funding

This work was supported by grants from the Incoming post-doctoral fellowships co-funded by the Marie Curie Actions of European Commission (Belgium) and the Back to Belgium Grant from the Belgian Federal Science Policy (BELSPO, Belgium).

Acknowledgement

The authors would like to thank Isabelle Habsch and Éric de Prez for providing technical assistance.

Additional information

This work was presented at the 51st ERA-EDTA Congress (31 May–3 June 2014, Amsterdam, The Netherlands) and at the Belgian Society of Physiology (Brussels, October 2014).

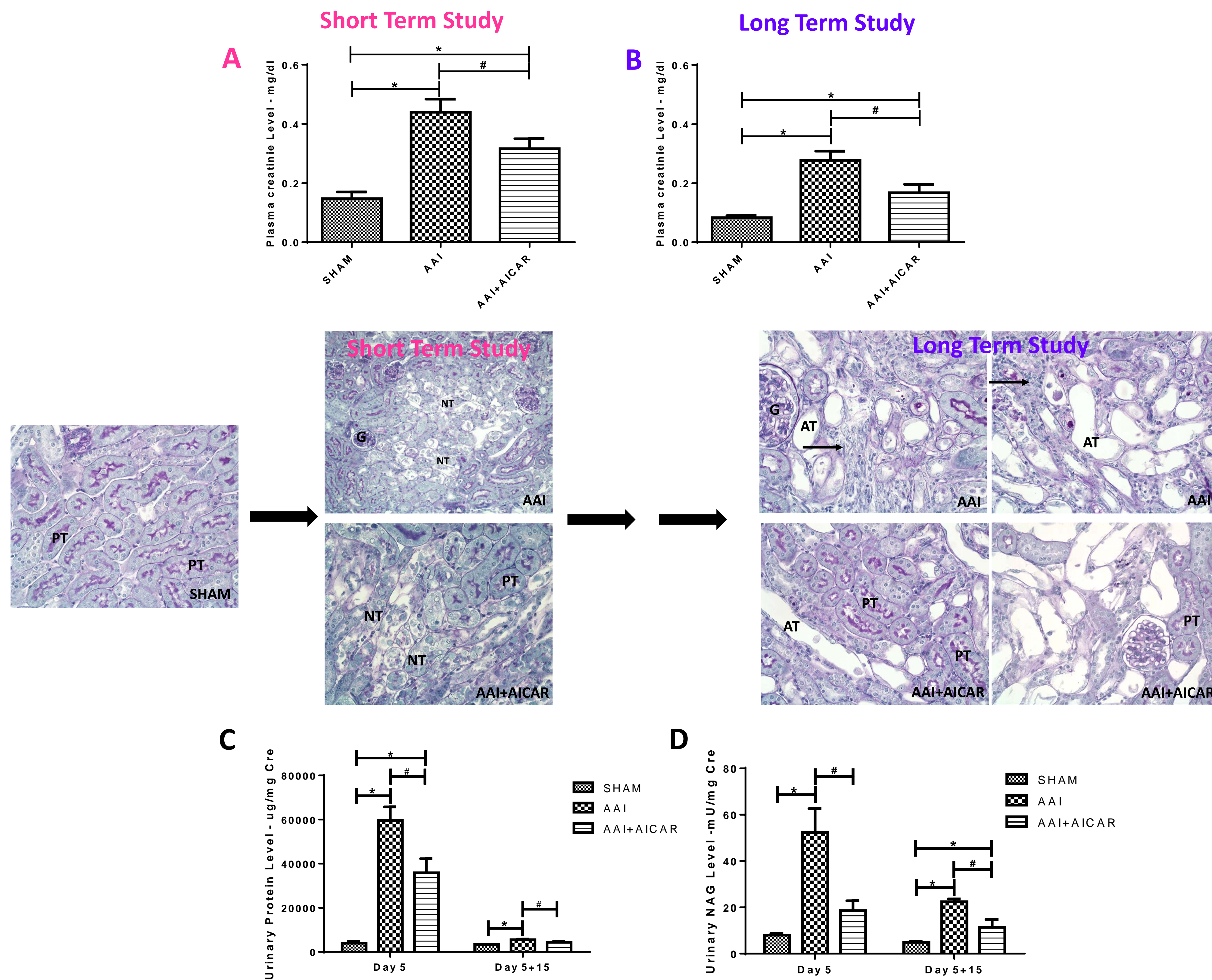
Background: Experimental aristolochic acid nephropathy (AAN) is a pertinent model of tubulo-interstitial nephritis characterized by an early phase of acute kidney injury (AKI) leading to progressive fibrosis and chronic kidney disease (CKD). Here, the present model was used to determine the role of AMPK in renal outcome and its involvement in the AKI-to-CKD transition.

1. Effect of AICAR treatment on body and kidney weights

Study	Group	Relative change in bw	Food Intake	Water Intake	Kidney Weight
		%	g/day	ml/day	g
Short Term Study	SHAM	4.90 ± 1.40	4.3 ± 0.2	6.8 ± 0.4	0.298 ± 0.015
	AAI	0.98 ± 1.02*	3.8 ± 0.3	6.0 ± 0.4	0.276 ± 0.003
	AAI+AICAR	3.29 ± 1.54	3.7 ± 0.4	6.1 ± 0.4	0.275 ± 0.004
Long Term Study	SHAM	7.56 ± 0.98	3.9 ± 0.1	5.0 ± 0.1	0.298 ± 0.015
	AAI	-4.14 ± 1.58*	3.7 ± 0.1	7.5 ± 0.4*	0.326 ± 0.007
	AAI+AICAR	0.00 ± 0.96*	3.3 ± 0.1	6.0 ± 0.5	0.302 ± 0.011

Values are means ± SEM. N=8 in each group. Statistical analyses were performed by one-way ANOVA followed by Newman-Keuls *p ≤ 0.05 versus SHAM mice and #p ≤ 0.05 versus AAI mice.

2. Effect of AICAR treatment on renal function and tubular structure

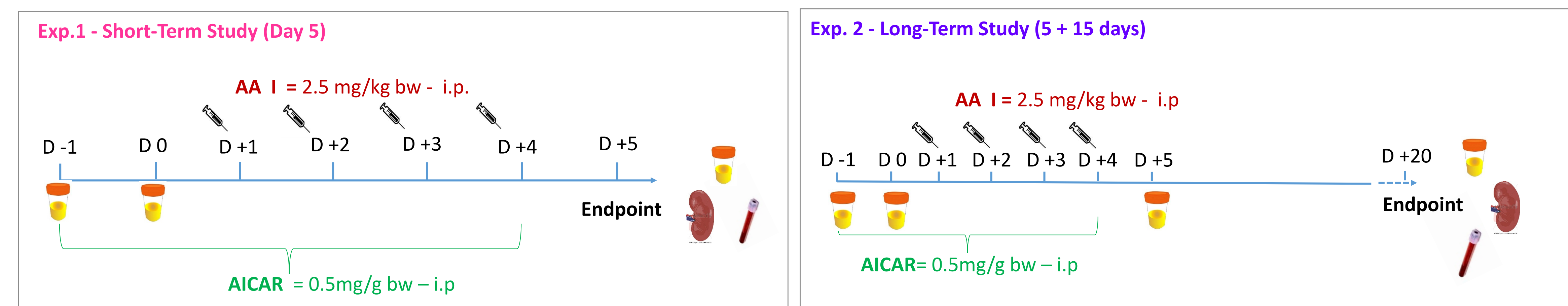


Quantitative plasma creatinine level in SHAM, AA and AA+AICAR mice at day 5 (A) and day 5+15 (B); Representative photomicrographs (x400) illustrating renal tissue injury with PAS staining in SHAM, AAI and AAI+AICAR mice at day 5 and day 5+15. Quantitative total urine protein level (C) and Quantitative urine NAG enzymuria level in SHAM, AAI and AAI+AICAR mice at day 5 and day 5+15.

Values are means ± SEM. N=8 in each group. Statistical analyses were performed by one-way ANOVA followed by Newman-Keuls *p ≤ 0.05 versus SHAM mice, #p ≤ 0.05 versus AAI-treated mice.

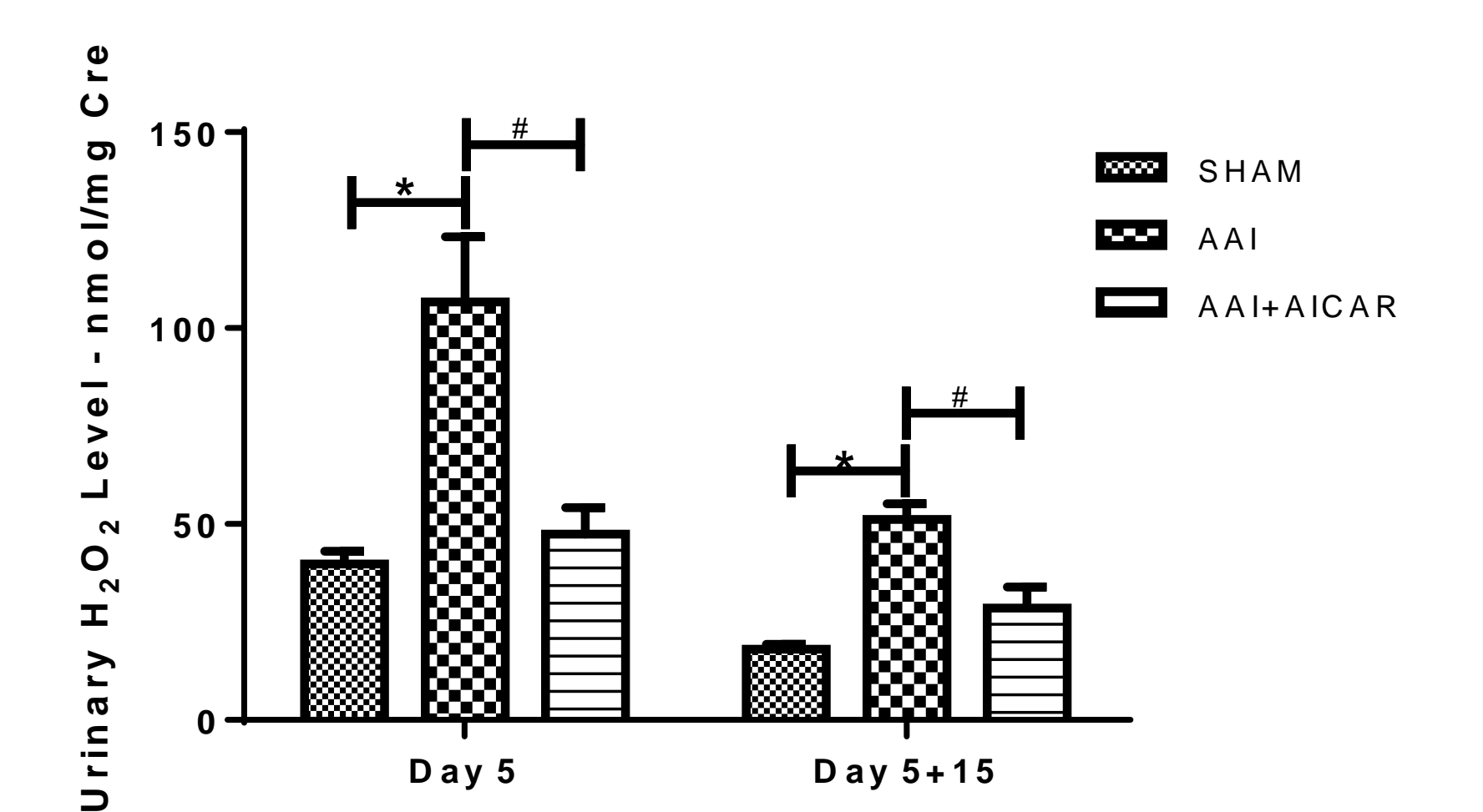
PT: proximal tubule; NT: Necrotic Tubule; AT: Atrophic Tubule; G: Glomerulus; Arrow: increase in infiltrated cells

Methods: C57BL/6J male mice were randomly subjected to i.p. injection of either sterile saline solution, AA, AA+AICAR (the specific AMPK activator) for 4 days. Mice were then euthanized either at day 5 (Exp.1) or day 20 (Exp.2).



3. Effect of AICAR treatment on oxidative stress

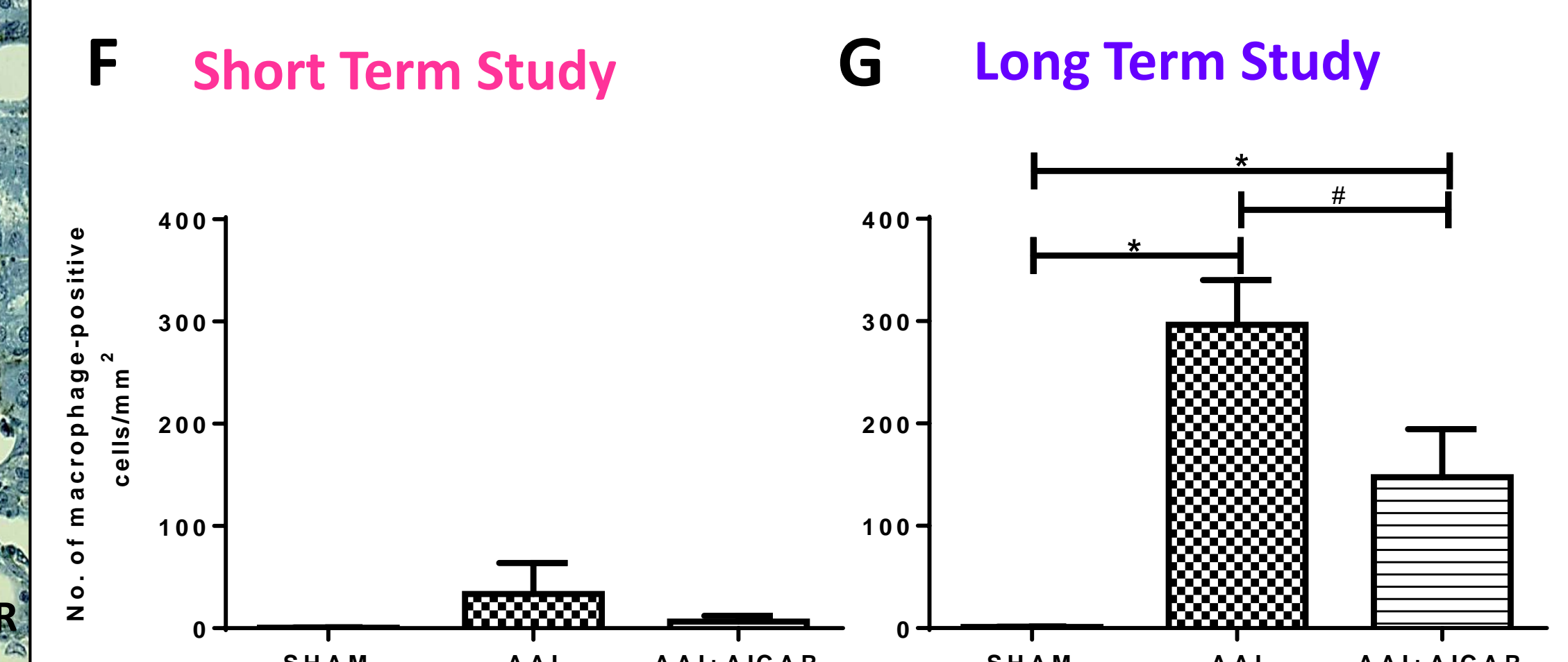
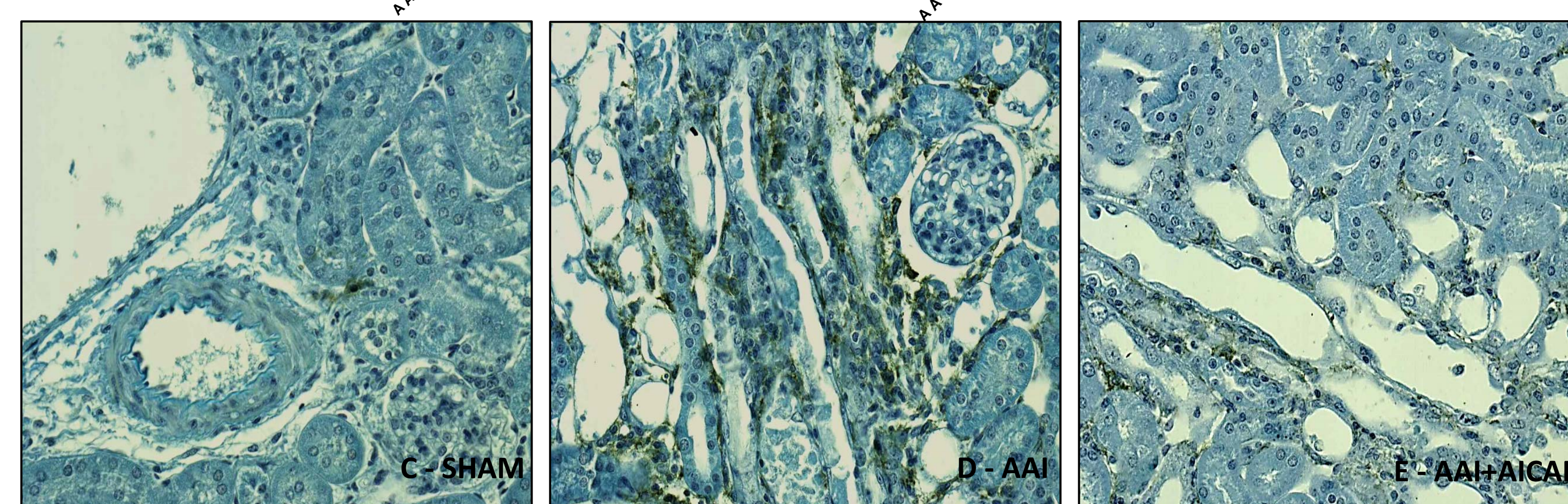
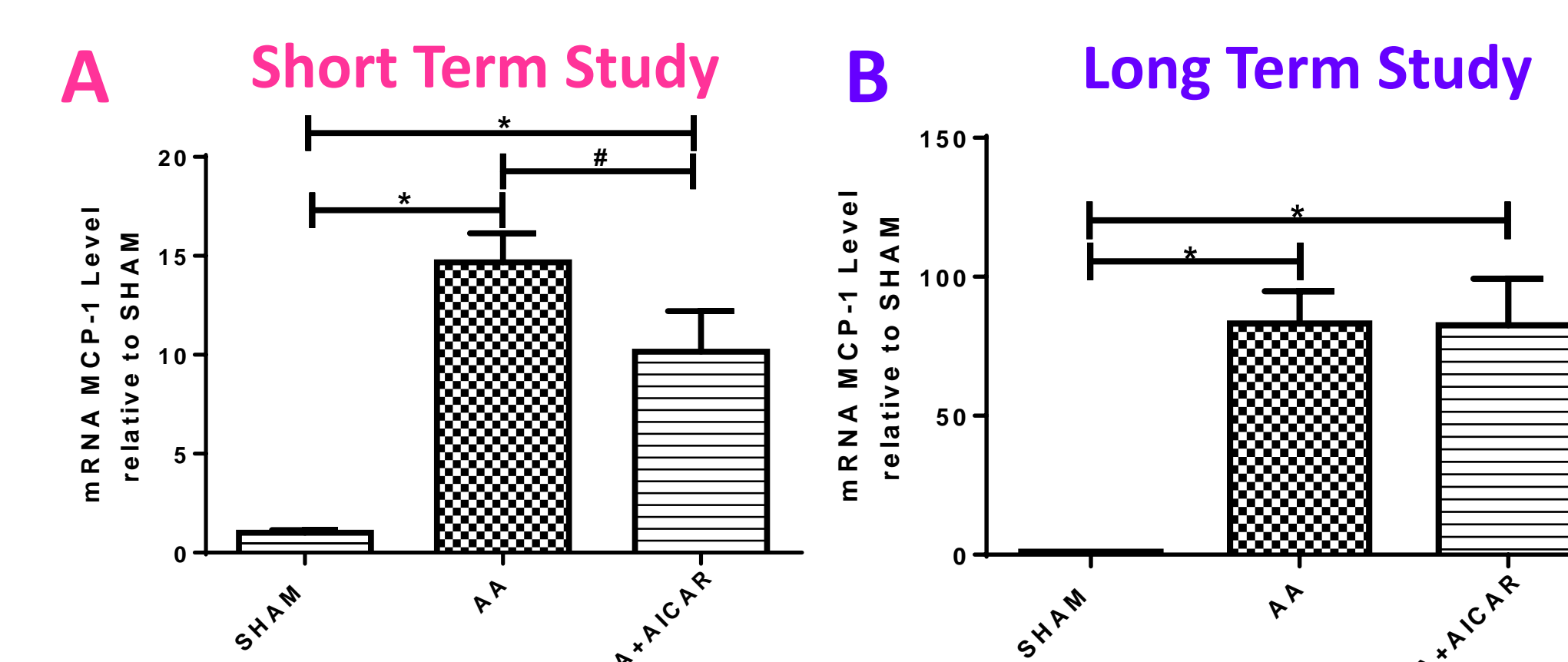
mRNA expression		Nox1	Nox2	Nox4
Short Term Study	SHAM	1.00 ± 0.26	1.00 ± 0.14	1.00 ± 0.15
	AAI	0.68 ± 0.16	2.20 ± 0.37*	1.25 ± 0.31
	AAI+AICAR	0.95 ± 0.24	1.06 ± 0.12#	1.22 ± 0.30
Long Term Study	SHAM	1.00 ± 0.34	1.00 ± 0.13	1.00 ± 0.18
	AAI	1.88 ± 0.69	28.12 ± 6.44*	0.56 ± 0.13
	AAI+AICAR	2.21 ± 0.49	23.38 ± 1.93*	1.36 ± 0.24



Quantitative real time PCR was performed with kidney from all groups each normalized against 18S.

Quantitative analysis of urine hydrogen peroxide (H₂O₂) level in SHAM, AAI and AAI+AICAR-treated mice. Values are means ± SEM. N=8 in each group. Statistical analyses were performed by one-way ANOVA followed by Newman-Keuls *p ≤ 0.05 versus SHAM mice and #p ≤ 0.05 versus AA-treated mice.

4. Effect of AICAR treatment on inflammation



Quantitative real-time PCR for MCP-1 mRNA expression was performed with kidney in SHAM, AA and AA+AICAR mice at day 5 (A) and day 5+15 (B). Representative photomicrographs (x400) illustrating macrophages (arrow) in SHAM (C), AAI (D) and AAI+AICAR (E) mice. Quantitative analysis of macrophage-positive staining in kidney tissue at day 5 (F) and day 5+15 (G).

SUMMARY

These findings show a beneficial effect of AMPK in AA-induced AKI. In view of these data, we suggest that chronic AICAR treatment is necessary for complete nephroprotection and recovery. The activation of AMPK represents a potential strategy to prevent the transition from AKI-to-CKD.

Email:

Anne-Emilie.decleves@umons.ac.be - Inès.jadot@unamur.be - joelle.nortier@ulb.ac.be

Implication of AMPK Activation in Experimental Aristolochic Acid Nephropathy. Use of a Targeted Metabolomic Analysis

AE Declèves^{1,3}, I. Jadot³, V. Colombaro³, B. Martin³, J. Naviaux², K. Li², N. Caron³, JL. Nortier¹ and RK. Naviaux²

¹Laboratory of Experimental Nephrology, Department of Medicine, Université Libre de Bruxelles (ULB), B-1070 Brussels, Belgium
²The Mitochondrial and Metabolic Disease Center, Department of Medicine, University of California, San Diego, CA, 92161, USA
³Molecular Physiology Research Unit-URPhyM, Department of Medicine, University of Namur, B-5000 Namur, Belgium

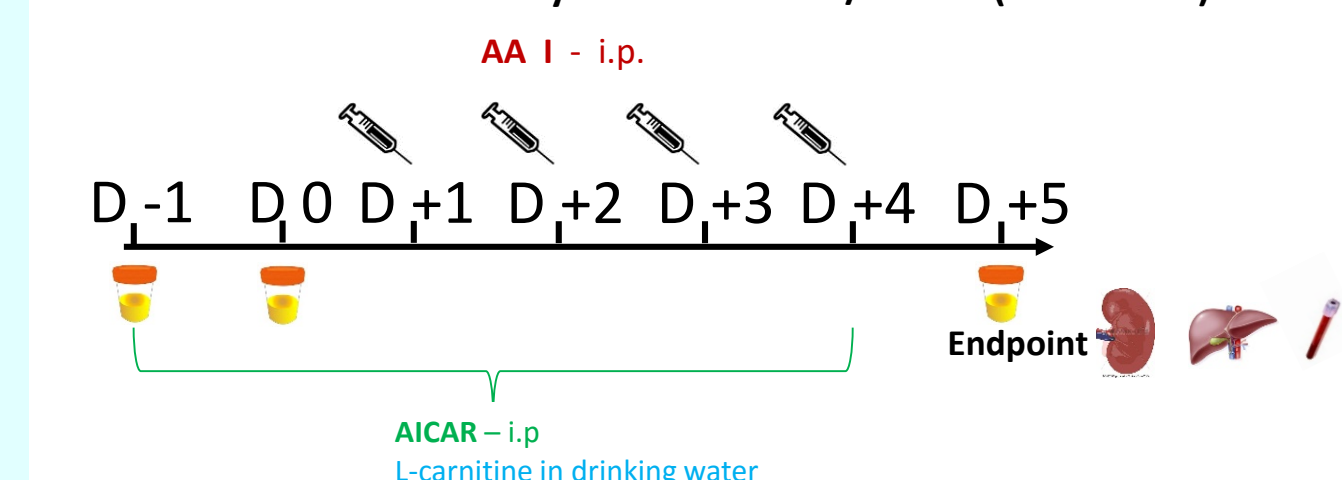
AIMS

Experimental aristolochic acid nephropathy (AAN) is a progressive tubulointerstitial injury, characterized by early and transient acute tubular necrosis. In order to better explore the pathogenesis of AAN, a targeted metabolomics analysis was performed in plasma of AA-intoxicated mice. In addition, the effect of AMP-activated Protein Kinase (AMPK) activation with AICAR was investigated by the use of AICAR alone or in combination with carnitine.

METHODS

C57BL/6J male mice were randomly subjected to i.p. injection of either sterile saline solution, AA, AA+AICAR, the specific AMPK activator for 4 days. Mice were then euthanized at day 5. Targeted metabolites were detected in plasma using an AB SCIEX QTRAP 5500 triple quadrupole mass spectrometer equipped with a Turbo V electrospray ionization (ESI) source, and Shimadzu LC-20A UHPLC system.

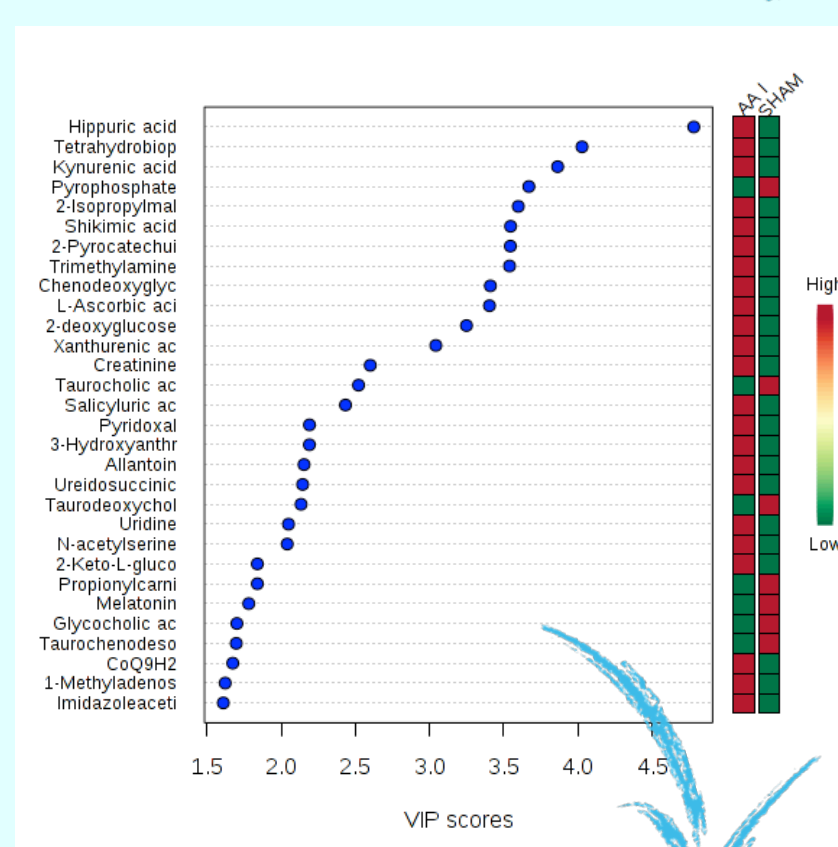
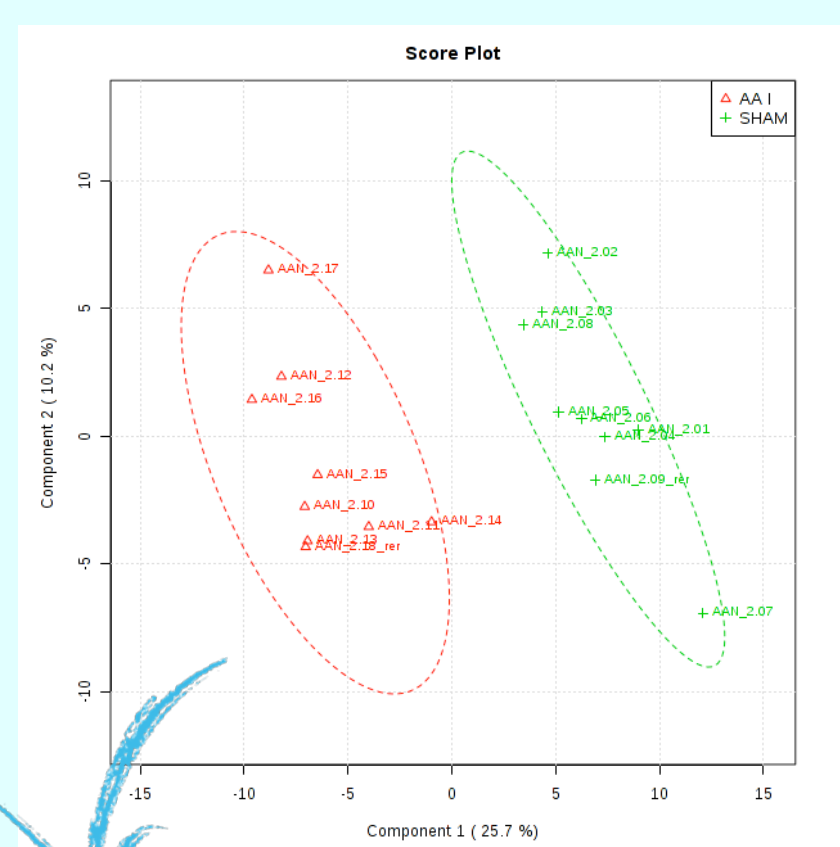
SHORT-TERM STUDY → 5 days → Male C57BL/6 Mice (8 week old)



Group I = Sham
 Group II = AAI (2.5 mg/kg) - 4 ip
 Group III = AAI (2.5 mg/kg) + AICAR (0.5mg/g) - ip
 Group IV = AAI (2.5 mg/kg) + AICAR (0.5mg/g) + L-carnitine (400mg/kg) in drinking water

RESULTS

I. COMPARISON BETWEEN SHAM AND AA-INTOXICATED MICE



Metabolites modified with AA	
SHAM - High	SHAM - Low
AAI - Low	AAI - High
Pyrophosphate	Hippuric Acid
Taurocholic Acid	Tetrahydrobiopterin
Taurodeoxycholic Acid	Kynurenic Acid
Propionylcarnitine	2-Isopropylmalic Acid
Melatonin	Shikimic Acid
Glycocholic Acid	2-Pyrocatechuic Acid
Taurochenodesoxycholic Acid	Trimethylamine
	Chenodeoxyglycholic Acid
	L-Ascorbic Acid
	2-deoxyglucose-6-phosphate
	Xanthurenic Acid
	creatinine
	Salicylic Acid
	Pyridoxal
	3-hydroxyanthranilic Acid
	Allantoine
	Ureidosuccinic Acid
	Uridine
	N-acetylserine
	2-keto-L-gluconate
	CoQ9H2
	1-Methyladenosine
	Imidazoleacetic Acid

Score Plot of partial least square discriminant analysis (PLS-DA) of plasma samples in sham (green) and AA-intoxicated (red) mice.

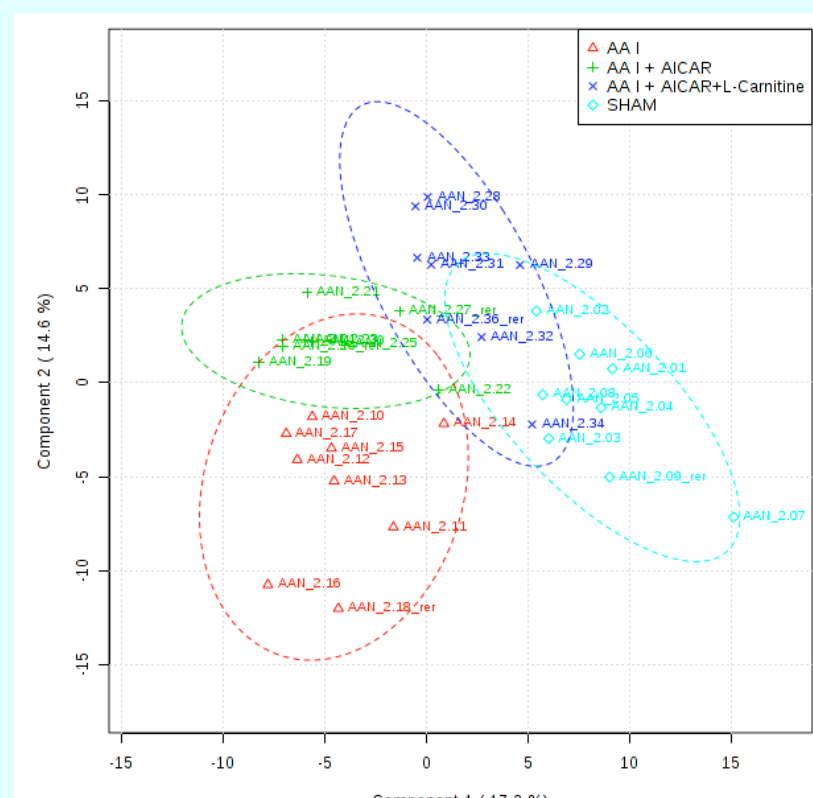
Top VIP scores with expression heatmap from PLS-DA models. PLS-DA models were constructed with signature metabolites from plasma samples of sham and AA-intoxicated mice. Red and green indicate increased and decreased levels, respectively.

Biochemical Pathways Altered by AA Compared to Sham

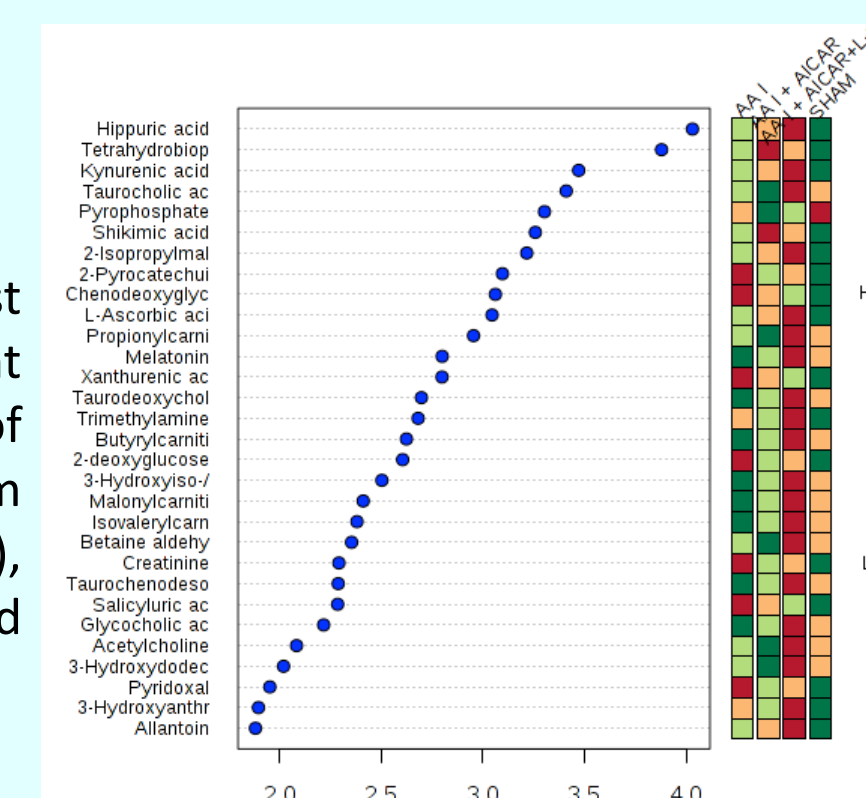
No.	Pathway Name	Measured Metabolites in the Pathway (N)	Expected Pathway Proportion (P = N/582)	Expected Hits in Sample of 35 (P * 35)	Observed Hits in the Top 35 Metabolites	Fold Enrichment (Obs/Exp)	Impact (Sum VIP Score)	Fraction of Impact Explained (% of 87,6403)	Increased (Exp/Clt-1)	Decreased (Exp/Clt+1)
1	Microbiome Metabolism	26	0.045	1.6	8	5.1	20.9	23.8%	7	1
2	Bile Salt Metabolism	7	0.012	0.4	5	11.9	11.5	13.1%	1	4
3	Tryptophan, Kynurenic, Serotonin, Melatonin	9	0.015	0.5	2	3.7	5.6	6.4%	1	1
4	Vitamin B6 (Pyridoxine) Metabolism	4	0.007	0.2	2	8.3	5.2	6.0%	2	0
5	Pyrimidine Metabolism	26	0.045	1.6	2	1.3	4.2	4.8%	2	0
6	Biopterin, Neopterin, Molybdopterin Metabolism	1	0.002	0.1	1	16.6	4.0	4.6%	1	0
7	Purine Metabolism	34	0.058	2.0	2	1.0	3.8	4.3%	2	0
8	Phosphate and Pyrophosphate Metabolism	1	0.002	0.1	1	16.6	3.7	4.2%	0	1
9	Phytanic, Branch, Odd Chain Fatty Acid	1	0.002	0.1	1	16.6	3.6	4.1%	1	0
10	Fatty Acid Oxidation and Synthesis	39	0.067	2.3	1	0.4	3.5	4.0%	1	0
11	Vitamin C (Ascorbate) Metabolism	3	0.005	0.2	1	5.5	3.4	3.9%	1	0
12	Pentose Phosphate, Gluconate Metabolism	9	0.015	0.5	2	3.7	3.4	3.8%	2	0
13	Glycolysis and Gluconeogenesis Metabolism	14	0.024	0.8	1	1.2	3.2	3.7%	1	0
14	SAM, SAH, Methionine, Cysteine, Glutathione	20	0.034	1.2	1	0.8	2.6	3.0%	1	0
15	OTC and Prescription Pharmaceuticals	1	0.002	0.1	1	16.6	2.4	2.8%	1	0
16	Isoleucine, Valine, Threonine, or Methionine	2	0.003	0.1	1	8.3	1.8	2.1%	0	1
17	Ubiquinone and Dolichol Metabolism	4	0.007	0.2	1	4.2	1.7	1.9%	1	0
18	1-Carbon, Folate, Formate, Glycine, Serine	5	0.009	0.3	1	3.3	1.5	1.8%	0	1
19	Branch Chain Amino Acid Metabolism	11	0.019	0.7	1	1.5	1.5	1.7%	0	1

RESULTS

II. EFFECT OF AICAR ALONE OR IN COMBINATION WITH CARNITINE IN AA-INTOXICATED MICE



Score Plot of partial least square discriminant analysis (PLS-DA) of plasma samples in sham (light blue), AA (red), AA+AICAR (green) and AA+AICAR+Carnitine (blue).



VIP scores with expression heatmap from PLS-DA models. PLS-DA models were created with signature metabolites from plasma samples of sham, AA, AA+AICAR and AA+AICAR+Carnitine-treated mice. Red and green indicate increased and decreased levels, respectively.

Metabolites modified with AICAR alone or with Carnitine in AA-intoxicated mice

SHAM - Low	AAI - High
2-Pyrocatechuic Acid	Microbiome Metabolism
Chenodeoxyglycholic Acid	Bile Salt Metabolism
2-deoxyglucose-6-phosphate	Glycolysis and gluconeogenesis Metabolism
Xanthurenic Acid	Pyridoxine (vit B6) Metabolism
Pyridoxal	Pyridoxine (vit B6) Metabolism
creatinine	SAM,SAH, Methionine, Cysteine, Glutathione Metabolism
Salicylic Acid	OTC/pharmaceutical Metabolism
Ureidosuccinic Acid	Pyrimidine Metabolism

Table including 8 metabolites that were low in SHAM and high in AAI. Both AICAR and AICAR in combination with carnitine reduced the level of these metabolites and prevented the AA effects.

CONCLUSIONS

These metabolomic approach provided novel findings regarding early perturbations occurring in metabolic pathways in AAN. Moreover, our results suggest 1) a crosstalk between gut microbiome and kidney, especially in relation with tryptophan metabolism and accumulation of uremic toxins; 2) a beneficial role of AMPK in reducing the level of uremic toxins.

Emails: Anne-Emilie.decleves@umons.ac.be – rknaviaux@ucsd.ac